April 1992 • NREL/TP-451-4797

Thin Film Cadmium Telluride Photovoltaic Cells

Annual Subcontract Report 23 July 1990 - 31 October 1991

A. Compaan
R. Bohn
University of Toledo
Toledo, Ohio

National Renewable Energy Laboratory
A Division of Midwest Research Institute
Operated for the U.S. Department of Energy
Under Contract No. DE-AC02-83CH10093

NREL/TP-451-4797 • UC Category: 273 • DE92001239

NREL/TP--451-4797

DE92 001239

Thin Film Cadmium Telluride Photovoltaic Cells

Annual Subcontract Report 23 July 1990 - 31 October 1991

A. Compaan
R. Bohn
University of Toledo
Toledo, Ohio

NREL technical monitor: B. von Roedern

National Renewable Energy Laboratory
(formerly the Solar Energy Research Institute)
1617 Cole Boulevard
Golden, Colorado 80401-3393
A Division of Midwest Research Institute
Operated for the U.S. Department of Energy
under Contract No. DE-AC02-83CH10093

Prepared under Subcontract No. ZN-1-19019-3

April 1992

On September 16, 1991 the Solar Energy Institute was designated a national laboratory, and its name was changed to the National Renewable Energy Laboratory.

Printed in the United States of America
Available from:
National Technical Information Service
U.S. Department of Commerce
5285 Port Royal Road
Springfield, VA 22161

Price: Microfiche A01
Printed Copy A03

Codes are used for pricing all publications. The code is determined by the number of pages in the publication. Information pertaining to the pricing codes can be found in the current issue of the following publications which are generally available in most libraries: *Energy Research Abstracts (ERA)*; *Government Reports Announcements* and Index (*GRA* and I); *Scientific and Technical Abstract Reports (STAR)*; and publication NTIS-PR-360 available from NTIS at the above address.

Summary

This program is pursuing the development of two vacuum-based growth techniques for CdTe thin-film solar cells. These are laser-driven physical vapor deposition (LDPVD) and radio-frequency (rf) sputtering. Most of the effort during the first year was devoted to the implementaton of LDPVD for CdS, CdTe, ZnTe, and $CdCl_2$ films and their integration into an efficient solar cell structure. In addition, after a mid-year contract renegotiation, a second growth technique, rf sputtering, was instrumented at the University of Toledo. This system became operational near the end of the first contract year.

To date, the LDPVD process has successfully been used for the deposition of thin films of CdS, CdTe, $CdCl_2$, as well as related alloys and doped semiconductor materials. The laser-driven deposition process readily permits the use of several target materials in the same vacuum chamber and thus complete solar cell structures have been fabricated on SnO_2-coated glass using LDPVD. The films require a second chamber only for the evaporation of metallization contacts. The all-LDPVD process with a heat treatment at 400°C for 40 minutes in air has resulted in an 8.7% AM 1.5 solar cell to date.

In addition to the efforts on optimization of the LDPVD process and the implementation of the rf sputtering process for film growth, significant efforts were devoted to the enhancement or implementation of a variety of film characterization systems and device testing facilities. Thus, by the end of the first year, we have been utilizing on a routine basis optical absorption, Raman scattering, photoluminescence, electrical conductivity, Hall effect, persistent photoconductivity, x-ray diffraction, and scanning electron microscopy with energy dispersive analysis. Finally important new information on the physical mechanisms of LDPVD has been obtained with a new system for transient spectroscopy on the ablation plume. These measurements have shown that, e.g., Cd is predominantly in the neutral atomic state in the plume but with a large fraction which is highly excited internally ($\geq$ 6 eV) and that the typical neutral Cd translational kinetic energies perpendicular to the target are 20 eV and greater.

Table of Contents

1.0 Introduction

1.1 Forward

This project began in July of 1990 as a joint project with the University of Toledo as the lead institution and the close participation of two lower tier subcontractors, Solar Cells Inc (SCI), and Glasstech Solar Inc (GSI). Near the end of 1990 GSI ceased operations and terminated its participation in the contract. Meanwhile, Solar Cells' time scale for moving toward module production advanced more rapidly than projected and NREL negotiated a separate contract with SCI in the spring of 1991. The contract with UT was renegotiated to reflect these changes with SCI remaining as a lower tier subcontractor only through the end of the first contract year. The time allocated for the first award year was extended through October 1991 to allow the University of Toledo to pick up some of the work initially planned for GSI. The University of Toledo contract was modified to reduce the second and third year emphasis on scale-up to commercialization, but retained the emphasis on basic science and the further development of the LDPVD and sputtering processes.

1.1 Technical Approach

The University of Toledo is, to our knowledge, the only research group using laser-driven physical vapor deposition (LDPVD) (also referred to as pulsed laser deposition or laser ablation deposition) for the growth of photovoltaic materials. The LDPVD process combines the advantages of (ultra)high vacuum cleanliness and monolayer control over the growth interface. It has many similarities to molecular beam epitaxy with much less cost. This growth process was studied intensively during the first contract year. We successfully fabricated by LDPVD complete solar cells with both CdS/CdTe and CdS/CdTe/ZnTe structures. The process included the use of LDPVD for the deposition of $CdCl_2$ prior to a heat treatment at 400°C.

With the departure of Glasstech Solar, the UT group also undertook the development of rf sputtering for CdTe thin-film growth and successfully deposited sputtered CdTe films by the end of October 1991. Coincident with this activity in studies of film growth, we implemented or improved on several techniques for thin-film materials characterization and for *in situ* diagnostics of the LDPVD and sputtering plumes. Finally, a considerable effort was devoted to the study of post-deposition processing and to the fabrication of complete solar cell structures.

2.0 Deposition Systems

2.1 Laser-Driven Physical Vapor Deposition (LDPVD)

Studies of the LDPVD process were begun at UT prior to the start of support from the SERI Polycrystalline Thin Films Initiative. This early work was supported by the State of Ohio's Thomas Edison Program, Solar Cells Inc., and The University of Toledo. NREL support has continued for the past 15 months of research effort as phase one of this project. We present here a basic description of the LDPVD system and a brief description of the deposition process.

The system for film growth is shown in Fig. 2-1 [1,2]. The 308 nm beam from the XeCl excimer laser (or 532 nm beam from the Nd:YAG) is weakly focussed with a 50 cm lens onto the pressed powder target. Target powders from Alpha Chemicals (five nines purity) were pressed in atmosphere to $\sim 3 \times 10^8$ Pascals before loading into the chamber. To prevent pitting and grooving of the target, the target holder was rotated in an oscillatory motion with a stepper motor from below. The laser spot was also moved in a radial oscillation using the mirror M1. An interior window W2 was heated to $\geq 350^{\circ}C$ to protect the laser entrance window from gradual accumulation of deposits. The elevated temperature and the high laser power density effectively prevent deposition on the inner window. Subsequent work showed that if the laser power density at the inner window exceeds ~ 0.1 J/cm^2 the window is self cleaning at room temperature.

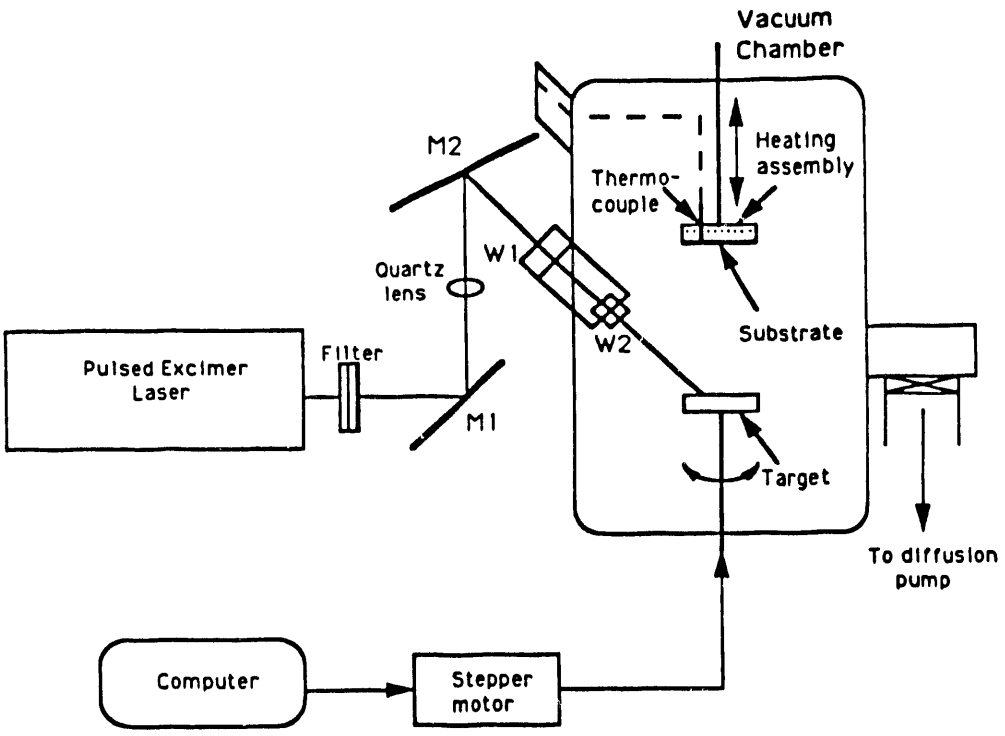

Fig. 2-1. Pulsed laser deposition system. M1 and M2 are mirrors, and W1 and W2 are quartz windows. The substrate is radiatively heated using a tantalum wire heater.

At focal power densities above ~3 J/cm^2, the laser pulse generates a plume of vapor oriented normal to the target surface with a half-width of about 9 degrees. The as-grown films were optically very smooth and usually free of pinholes. Because of the thickness variation away from the point normal to the target laser interaction spot, it was convenient to obtain the film thickness profile simply by scanning a focussed AlGaAs laser spot (λ=840 nm) or a HeNe laser (λ = 632.8 nm) along the film and recording the reflected intensity. Fig. 2-2 translates the interference fringe results for a CdS film into an angular dependence for the laser-driven plume. Note that the results are displayed for two scans--one parallel and one perpendicular to the plane of incidence of the excimer laser and the target. The film thickness has essentially circular symmetry and follows a Gaussian shape over the central 70% but falls more slowly in the wings of the deposition.

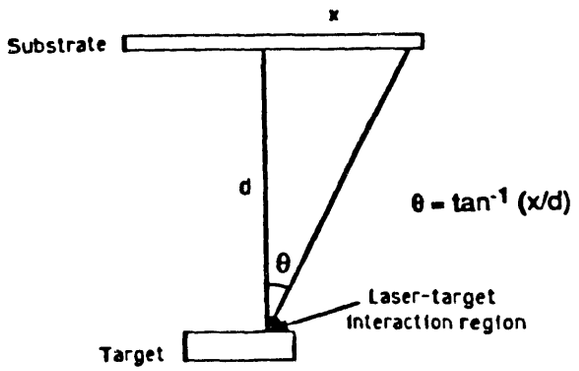

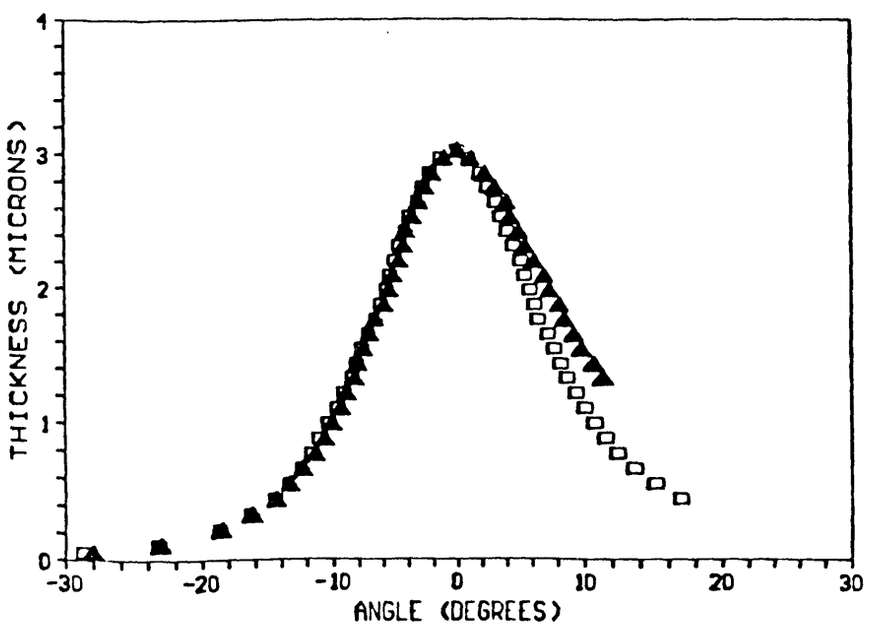

Fig. 2.2 Angular dependence of film thickness.

The efficiency of target utilization was measured by directly weighing the target and substrate before and after a deposition. We find that at a typical substrate growth temperature of 260°C, 40% of the mass lost from the target appears as film on the two-inch square substrate. For a room temperature substrate, about 55% of the target mass loss appears as deposited film. The above results were obtained for a target-substrate separation of 55mm, a laser power density of ~ 5 J/cm^2, and a vacuum pressure of $\sim 5 \times 10^{-6}$ Torr. At laser power densities of ~ 5 J/cm^2 for CdTe, the growth rate at the center of the deposition was about 1 Å per pulse. Further details of the physics of the LDPVD process are given in Section 4.1 below.

2.2 Radio Frequency Sputtering

The original project plan called for Glasstech Solar to pursue studies of rf sputtering of cadmium telluride. In the revised plan, this phase of the project was instrumented at the University of Toledo.

The rf sputtering system is sketched in Fig. 2-3. It utilizes the 13.57 MHz generator and power monitor from a GSI-built plasma CVD system. A new Π-network impedance matching system was constructed and a 2 inch diameter magnetron sputter gun (AJA International) was installed in a stainless steel turbo-pumped vacuum chamber. The substrate holder is radiatively heated with a tantalum wire heater. Base pressure in the chamber is $\sim 3 \times 10^{-7}$ Torr. The target material was pressed and sintered CdTe prepared from 5N purity powder (Angstrom Sciences).

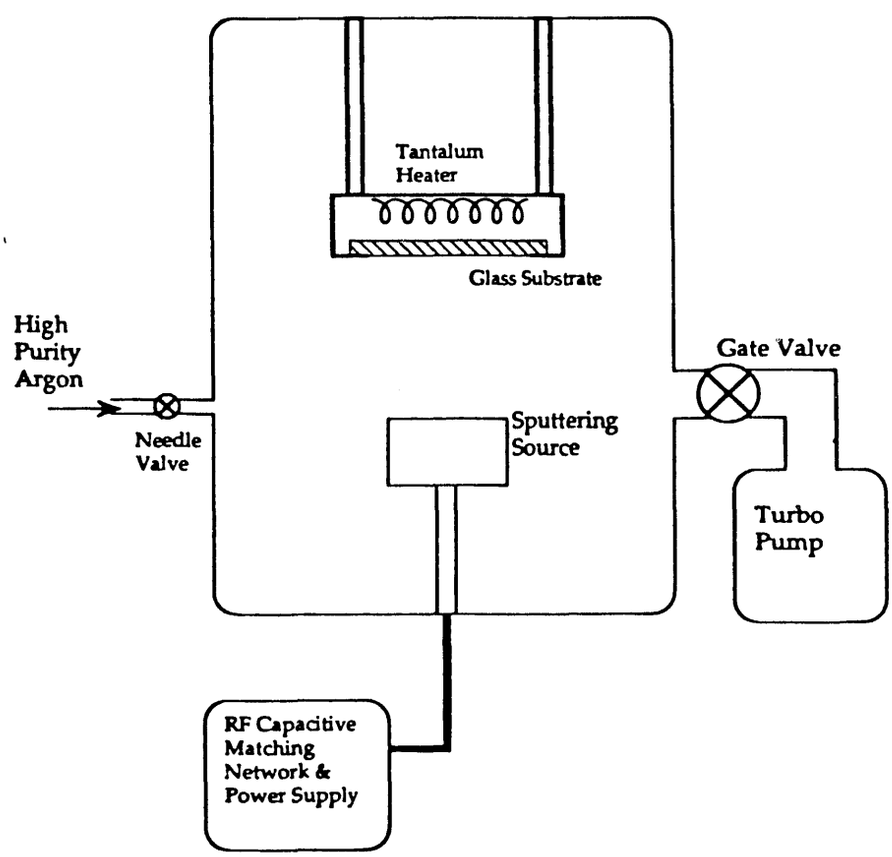

Fig. 2-3. RF sputtering system.

2.3 *In Situ* Diagnostics of LDPVD

The physical mechanisms of the laser-driven deposition process are not yet well understood. Therefore we have instrumented a system for optical studies of the laser-driven plume as well as of the sputtering plasma. This affords the opportunity for comparisons between the two processes. In the case of the LDPVD system, since it is initiated with a short (~15 nsec) pulse it is relatively easy to perform optical time-of-flight measurements to measure the translational kinetic energies of the atoms and ions which are light emitters. This system is based on an Aries FF250 1/4 meter spectrometer which can be operated with a photomultiplier for time-resolved measurements. A second exit port is fitted with a PAR OMA-II optical multichannel detector. This vidicon-based system is ideal for spectroscopy of transient, high-intensity phenomena.

2.4 Post-Deposition Treatment

Individual films and solar cells were annealed in a Thermco MINI-BRUTE Research Diffusion Furnace, Type MB-71. Its operating range is 400°C - 1300°C, but it has been modified to operate between 200°C - 1100°C. There are three zones of temperature control and the furnace is designed to provide a continuous flow of gas with a pre-set composition during sample annealing.

Application of thin layers of $CdCl_2$ was done in either of two methods. The first utilized the technique described by the Institute for Energy Conversion with drops of a solution of $CdCl_2$ in methanol. The second method utilized the laser deposition process. We found the LDPVD method to be more reliable especially since it could be performed in the same vacuum chamber as used for the depositions of CdS and CdTe without exposing the films to air.

2.5 Contact Application

Contact application was performed in a vacuum bell jar with thermal evaporation boats using elemental sources of gold, copper, or nickel.

3.0 Materials Characterization Systems

3.1 X-ray Diffraction

The x-ray diffraction studies were performed on a Scintag XDS 2000 instrument using a theta-theta configuration in which the sample plane remains stationary at the horizontal while the x-ray tube and detector move through angles of θ and $-\theta$. We used Cu k_α radiation with the tube operated at 45 kV and 40 mA. A cooled germanium crystal was used for detection. Normal resolution was 0.3 degrees but occasionally the system was used with narrower slits to achieve a resolution of 0.1 deg. Software provided the ability to do routine $k_{\alpha 2}$ stripping from the spectra.

3.2 Optical Absorption

Optical absorption measurements were performed on a Varian DMS300 double beam spectrometer using typically 1 mm apertures immediately in front of the sample films. Transmission and absorbance could be digitized for later analysis.

3.3 Raman and Photoluminescence

Raman scattering was performed on an ISA triple spectrometer (DHR320 + HR640) at both room temperature and at liquid nitrogen temperature. A few results have been obtained at liquid helium temperatures. The excitation sources were either a Lexel argon ion laser (λ = 514.5, 488.0, 476.5, and 457.9 nm) or a Lexel krypton ion laser (λ = 647.1, 676.4, and 752 nm). Detection was with a cooled GaAs photocathode photomultiplier and photon counting electronics.

3.4 Scanning Electron Microscopy and Energy Dispersive Spectroscopy (SEM/EDS)

The scanning electron microscope used in these studies was a JEOL Model JSM-6100. Typical working distances were 12 mm or less and accelerating voltages ranged from 5 kV to 30 kV. Studies of single films used glass substrates with nominal film thicknesses of 1 μm. Samples were sputter-coated with either carbon or gold prior to insertion in the SEM vacuum chamber. In some cases, the samples were chemically etched prior to carbon/gold deposition to improve grain boundary definition.

The SEM system is equipped with an eXL x-ray energy dispersive spectrometer (EDS) from Link Analytical. eXL is a multiprogram, multitasking instrument with Si/Li detectors specified at better than 133 eV resolution. All samples studied by EDS were coated with a carbon film. When compositional comparisons were made to a standard sample, care was taken to maintain identical microscope operating conditions for the samples.

3.5 Conductivity and Hall Systems

Conductivities were measured using a four-point probe (Alessi C4R), a Keithley Model 225 current source, and a Hewlett Packard 6217A power supply. Voltages were read with a Keithley 193 System digital multimeter and a Fluke 8840A multimeter. A Keithley Model 617 programmable electrometer was also used. Generally these instruments were used in a four probe configuration for the measurement of room temperature conductivities.

Most of the conductivities (particularly those as a function of temperature) were determined using a low temperature Hall system dewar from MMR Technologies, Inc. and a Van der Pauw configuration. Samples were mounted on a cold stage in a vacuum where the temperature could be varied from 80 K to 350 K. The cold stage was cooled by a miniature Joule-Thomson refrigerator using nitrogen gas. All electrical leads were Triax.

Hall measurements were done in the same system using a small magnet with maximum field of ± 4.0 kG. This system, as well as the Van der Pauw system, was completely computer controlled.

3.6 Current-voltage (I-V) System

Current-voltage measurements were made on completed solar cell structures in the dark and with tungsten halogen illumination (ELH lamp) equivalent to AM 1.5. The system utilized a D/A interface card for setting voltage and the current was read with a Philips model 2525 multimeter controlled by an IEEE GPIB interface.

3.7 Spectral Quantum Efficiency

An ELH lamp with a Spex 1/4 meter monochromator served as the light source for the spectral quantum efficiency measurements. The system was calibrated directly using a disk calorimeter (Scientech model 36001) and then referenced to a crystalline silicon cell which served as a convenient normalization standard.

4.0 Film Growth and Materials Quality

4.1 CdS

4.1.1 Film growth using Nd:YAG and excimer lasers (plume spectroscopy)

The LDPVD process is driven, in most of our work, by an XeCl laser pulse (~15 nsec, 308 nm, ~3 J/cm^2) from a pressed powder target. The intense laser pulse generates dense vapor which rises perpendicular to the target surface in a narrow plume and deposits onto a substrate heated to ~280°C. The plume consists mostly of uncharged atomic, a few ionic, and possibly some molecular species. We have used optical spectroscopy of the plume to determine translational velocities and characteristic temperatures in the vapor. Fig. 4-1 shows a spectral region which has three prominent lines identified with neutral Cd atoms. These data were obtained with the 1/4 meter spectrometer/vidicon system described in Section 2.3 above. The upper trace was taken at the point of interaction of the laser pulse and the target. The lower trace was obtained from a region ~ 4 mm above the target. The broadening apparent in the upper trace arises probably from collisions in the dense, hot vapor immediately above the target. The upper state for all three of these lines is the configuration 5s6s ($^3S_1$) which lies 6.38 eV above the ground state of the Cd atom.[4,5] This implies that a considerable amount of internal excitation occurs in at least some of the vapor constituents.

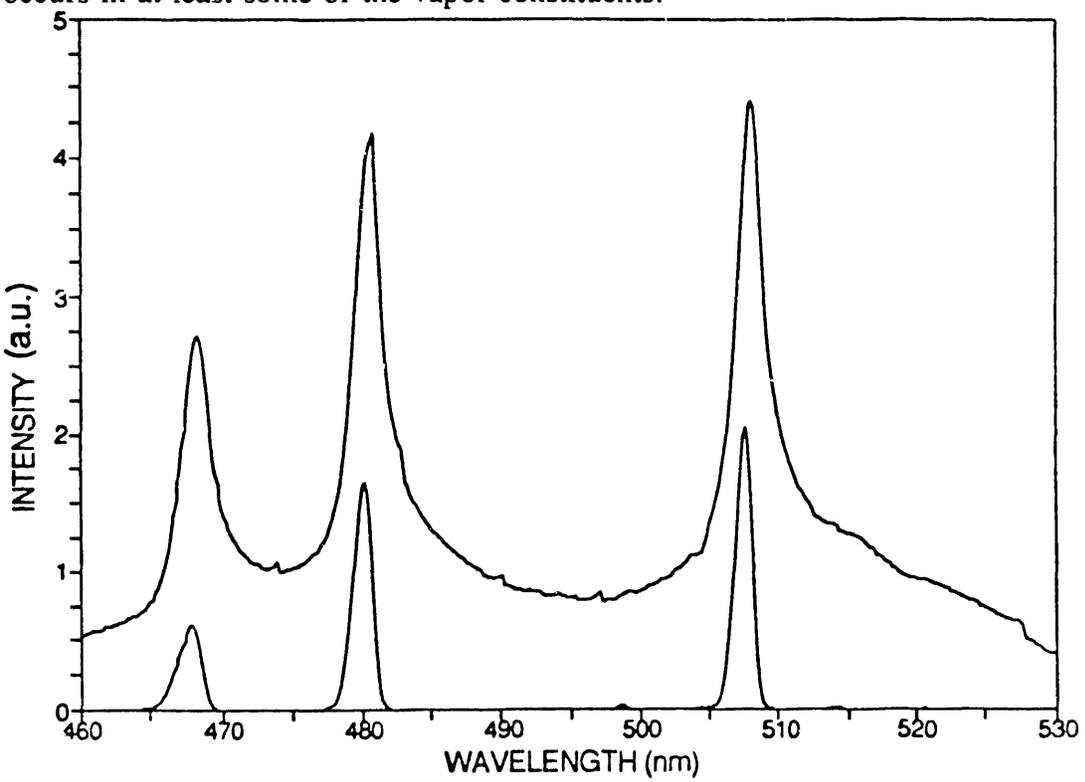

Fig. 4-1. Spectra of optical emission from an excimer laser-driven plume from a CdS target. The three peaks at λ = 4680 Å, 4800 Å and 5080 Å arise from transitions in neutral cadmium atoms. Upper trace imaged from the target surface; lower trace ~4mm above the target.

We also have made time-of-flight measurements by time-resolving the plume light emission with a photomultiplier and a digitizing oscilloscope. Fig. 4-2 shows two traces obtained with the spectrometer centered on the 480 nm Cd emission line. One may easily convert this temporal trace into a curve of velocity probabilities since the time origin is well defined. (See the top trace in Fig. 4-2.) The resulting velocity probability distribution is plotted in Fig. 4-3. Here the solid curve has the functional form[4].

$$f(v) = (8/3\pi)(m/2kT)^{5/2}\, v^4 \exp(-mv^2/2kT). \quad \text{Eq. 1}$$

[The v^4 prefactor arises from a uniform spatially diverging expansion ($1/r^2$) and from the conversion from temporal to velocity probabilities.]

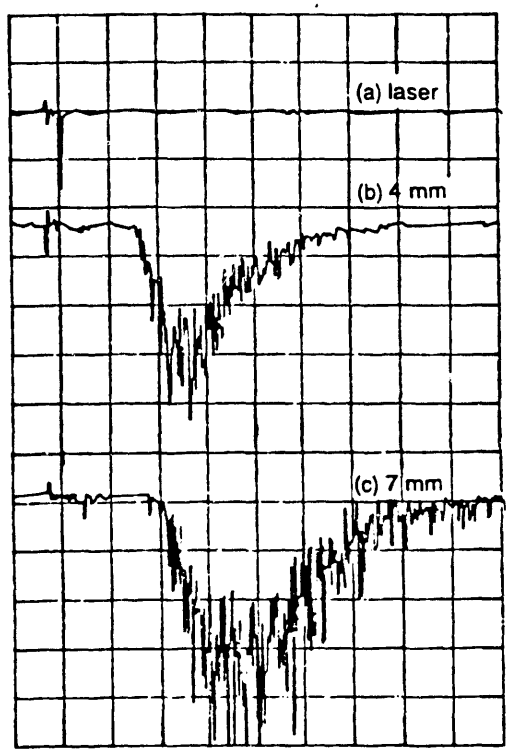

Fig. 4-2. Intensity of the λ = 4800 Å emission; (a) laser pulse, (b) 4 mm and (c) 7 mm above laser-target interaction region; horizontal: 500 nsec/div.

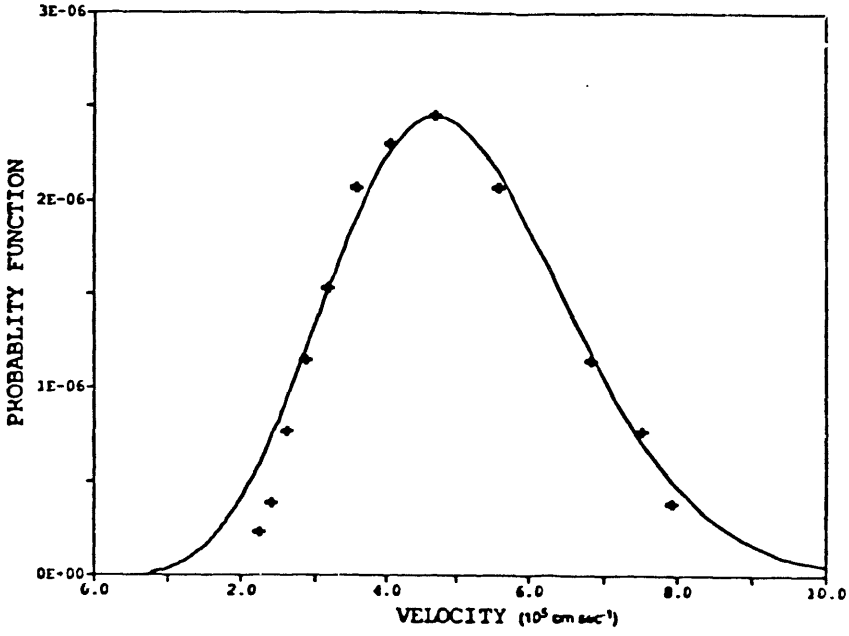

Fig. 4-3. Distribution of the vertical components of the velocities of neutral cadmium atoms. Solid curve from Eq. 3 with T = 70,000K.

Although there is some discrepancy in the low velocities, the overall fit is quite good for a plume translational temperature of 75,000 K (in the direction perpendicular to the target). This corresponds to typical kinetic temperatures of 5-10 eV in the plume. These conditions are quite different from the temperatures of ≤ 1000 K which obtain in the case of closed space vapor transport or other near equilibrium evaporative techniques. Spray pyrolysis, electrodeposition, and metal-organic chemical vapor deposition (MOCVD) utilize temperatures of typically 400°C or below. On the other hand, sputtering will typically generate kinetic energies of ~ 100 eV or more. Thus LDPVD opens an interesting intermediate kinetic energy regime for thin-film growth.

Fig. 4-4 summarizes some of the parameters important for the laser deposition process. The quantity of evaporated or ablated material begins from nearly zero at 0.5 J/cm^2 and rises approximately linearly with laser power until ~ 3 J/cm^2 beyond which the material loss saturates. The light intensity monitored at 480 nm rises rapidly with laser power above ~ 2 J/cm^2 and the neutral atom (Cd) kinetic energy similarly rises with increasing pulse energy. From these data one may infer that the pulse energy for most efficient target utilization is approximately 3 J/cm^2. Above 3 J/cm^2 additional laser energy simply appears as additional kinetic energy of the plume constituents.

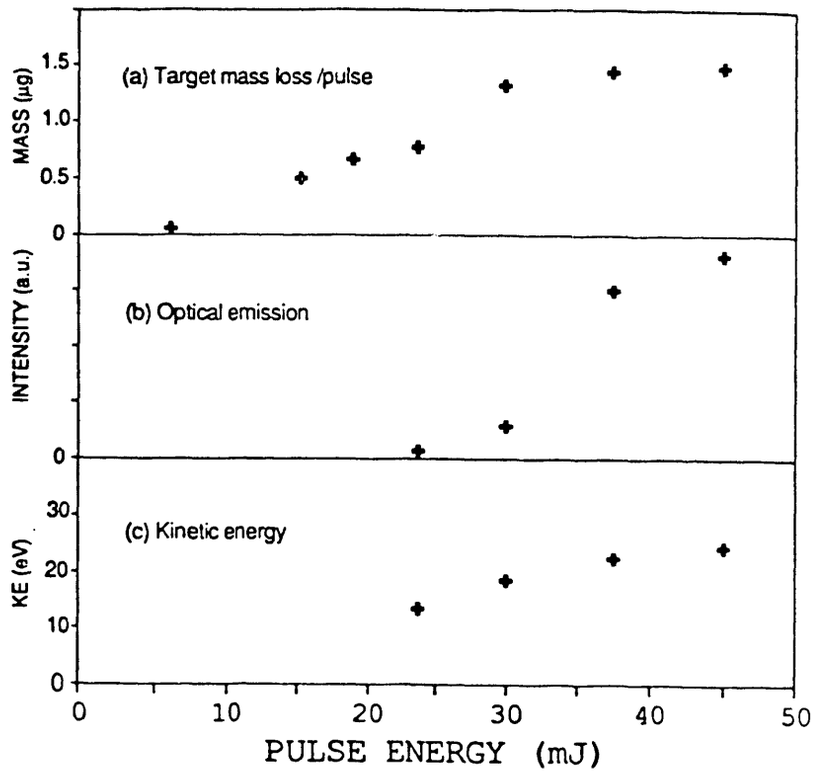

Fig. 4-4. Dependence of (a) target mass loss per pulse, (b) peak emission intensity at 480 nm, (c) kinetic energy on laser pulse energy. The laser spot size on the target was ~ 1 square mm.

4.1.2 Grain size and orientation

During the past year, we have studied the materials properties of the CdS films by x-ray diffraction, optical absorption, Raman scattering, and by electrical measurements. Highlights of the results are presented below.

X-ray Diffraction--Crystalline CdS has either the hexagonal zinc sulfide (wurtzite) or the cubic zinc sulfide (zinc blende) structure, although the wurtzite is the stable phase at room temperature. Fig. 4-5 shows some results for a CdS film. Laser pulse energy density was ~3 J/cm^2 with a target-to-substrate distance of 55 mm. The x-ray peaks at ~26.50 degrees can arise from either the hexagonal structure with the c-axis oriented perpendicular to the substrate or the cubic structure with the <111> direction perpendicular to the substrate. The limited resolution of the spectrometer does not allow us to distinguish between these two structures. However, the x-ray data do confirm that the preferential c-axis or <111> orientation increases as the substrate temperature increases. The predominant polycrystalline grain orientation was <002> (or <111>) for growth temperatures of 180°C and above.

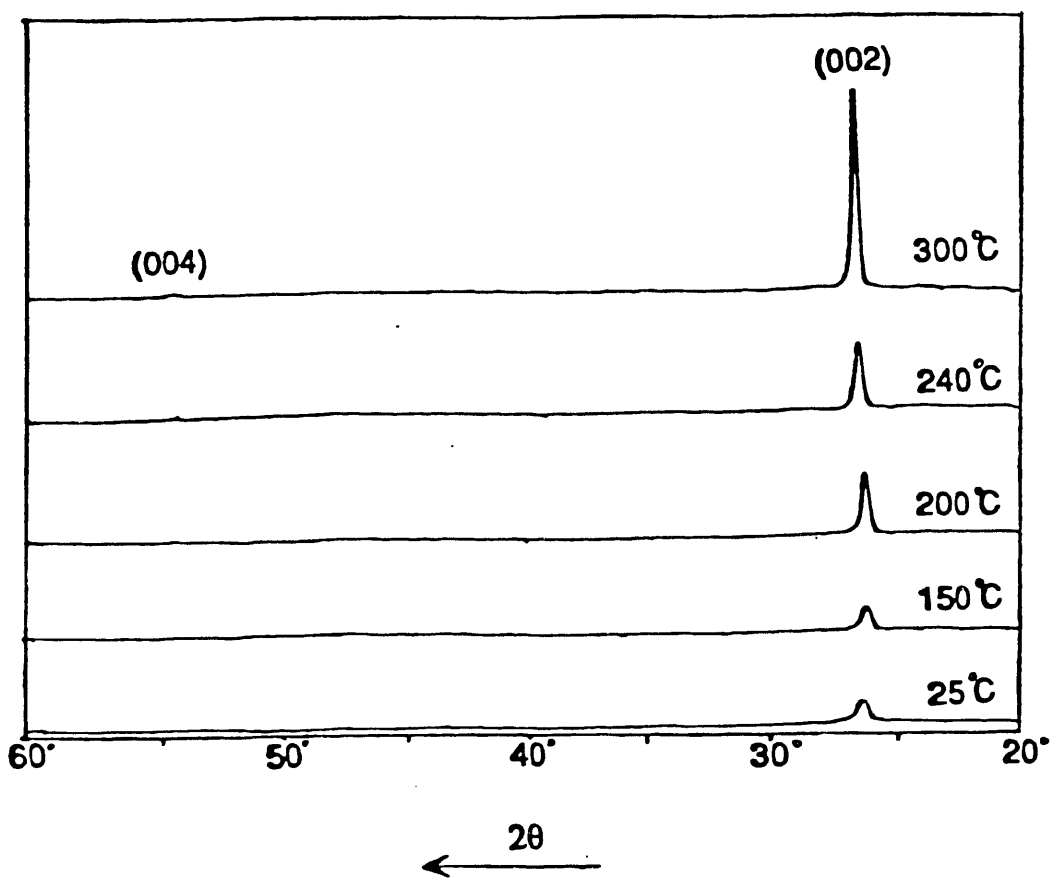

Fig. 4-5. CdS x-ray data for films deposited at different temperatures.

The full widths at half maximum (FWHM) were typically of the order of 0.3 degrees (very close to the normal instrumental resolution) and decreased as the substrate temperature increased. Since the FWHM depends on several parameters; i.e., grain size, defects, and strain, no attempt was made to determine the grain size from the x-ray FWHM.

SEM Studies--The short circuit current density, open-circuit voltage, and fill factor can all be strongly influenced by electron-hole recombination which can occur at grain boundaries in polycrystalline layers[6]. Post-growth treatment of CdS/CdTe solar cells with $CdCl_2$ has been done for several years to improve efficiency[7]. Either the individual layers, or the cell itself, have been subjected to this treatment. For example, the sintering of CdS films which contain $CdCl_2$ produces films of higher density and promotes grain growth[8]. Since the SEM evidence suggests that the as-deposited films had relatively small grain sizes ($\sim$ 100-1000 Å), the CdS and CdTe films were subjected to various post-growth treatments in an effort to promote recrystallization and grain growth. These included the mixing of $CdCl_2$ with target materials, the more traditional $CdCl_2$ -methanol treatment [2], and a laser-deposited $CdCl_2$ overlayer. Some of the results of these post-growth treatments will be presented in this and later sections.

SEM and EDS studies were performed on as-grown and treated samples. The average grain diameter was estimated by counting the number of grains that intersected a line of given length that was superimposed on the SEM photograph. This number was then divided by this scaled length to determine the number of grains per μm.

In order to study the effects of the $CdCl_2$ treatment and post-growth anneal on the laser-deposited films, CdS was deposited on glass and then a $CdCl_2$ layer was laser-deposited over the CdS. Samples were then annealed in air for 30 minutes at various temperatures and the grain size was compared to the as-grown samples. Table 4-1 lists the results. Little grain growth is seen until an annealing temperature of 400°C is reached. The data suggest that at temperatures greater than 450°C the average grain size increases by a factor of three to four and that temperatures greater than 500°C could be used for the largest effect. However, temperatures greater than about 500°C produce sublimation of the CdTe film, so studies were not continued on CdS beyond this temperature.

The EDS spectra for CdS were used to compare the composition of a CdS standard (a single crystal) to that of a film. In the EDS studies the spectral intensity ratios from a standard sample were compared to those from the film. The ratio of the intensity of $S_{K\alpha}$ to $Cd_{L\alpha}$ was 1.069 for the standard. The corresponding ratio for the film was 1.076. We conclude that the S/Cd ratio of the film is the same as that of the reference sample within the experimental error of $\pm 1\%$. SEM studies show that the grains are columnar with lengths extending through the typically 1 μm film thickness and with diameters $\sim$500Å prior to annealing.

Table 4-1. Grain size of a 0.6 μm CdS film treated with $CdCl_2$. (T = annealing temperature, R = range of grain diameters, and n = number of grains per μm).

T (°C)	R (μm)	n (μm^{-1})
500	0.2 - 0.6	2.4
450	0.1 - 0.3	6
400	0.05 - 0.3	10
350	0.05 - 0.1	13
as grown	0.05 - 0.1	13.5

4.1.3 Optical properties

Optical absorption measurements obtained with the double beam spectrometer for films deposited on Corning 7059 glass indicated absorption edges (extrapolated from plots of α^2 vs $h\nu$) typical of crystalline films as reported in the literature for both CdS and CdTe. The optical absorption was found not to be as sensitive to the crystal quality as the other measurements discussed here.

Raman scattering was performed on both CdS and CdTe films and provided results which were quite sensitive to the film quality. For CdS the Raman scattering was obtained with an argon laser line (λ = 457.9 nm) with a photon energy slightly above the CdS band gap. In this case the (resonant) Raman effect is similar to a resonance photoluminescence process[4] in which the photoexcited carriers may scatter from one optical phonon (first order Raman) or from two or more optical phonons (Raman overtones) before undergoing radiative recombination. However, the photoexcited carriers (electrons or holes) may also scatter from impurities or recombine nonradiatively. These competing processes will decrease the intensity of the higher order Raman lines relative to the first order Raman process. This behavior is seen in Fig. 4-6 in which one may observe the room temperature first, second, and third-order Raman lines from a bulk single crystal, and from two polycrystalline CdS thin films grown at 215°C and 260°C. Note that the results from the 260°C film deposition are significantly better than for deposition at 215°C but still show less overtone intensity than the bulk single crystal. (The background at the larger frequency shifts arises from the near-band-edge photoluminescence due to thermalized carriers.)

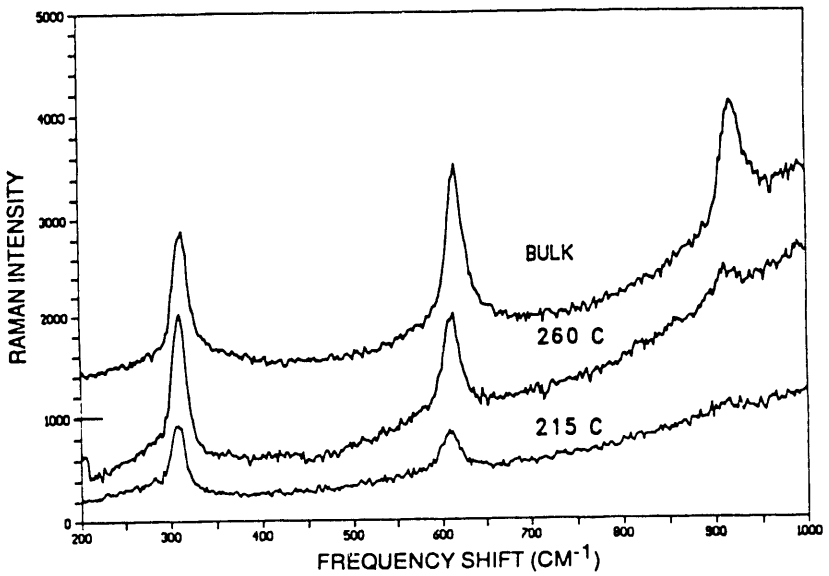

Fig. 4-6. Raman scattering spectra showing the first order LO phonon at ~300 cm^{-1} and two overtones for bulk single crystal (baseline shifted by 1000 counts) and for two polycrystalline films with different growth temperatures. Raman excitation: λ = 457.9 nm.

4.1.4 Electrical transport properties

Effect of Substrate Temperature on Doping--Dark resistivities were measured of several as-grown films all of which had 500 ppm of indium in the target material during growth. CSG-15 and -26 were deposited at a substrate temperature of 210°C and CSG-19 had a substrate temperature of 260°C. At this doping level, the resistivities are essentially independent of temperature near room temperature. Hall effect studies show that the mobility follows an activation energy model,

$$\mu = \mu_o e^{-E/kT} \tag{4-2}$$

which is to be expected for polycrystalline films where the barriers at the grain boundaries dominate the conductivity. In the vicinity of room temperature, the slope of a semi-log plot of μ vs. 1/T yields an activation energy for the mobility of the order of 70 meV. Carrier concentrations are 10^{16} - $10^{17}/cm^3$. Thus, for CdS grown on glass, the transport properties (mobility and carrier concentration) appear not to have much sensitivity to substrate temperature near 300 K. It should be noted that only a few percent of the indium appears to be activated if the concentration is near the target concentration of 500 ppm (~ $10^{19}/cm^3$). This effect has been reported by other researchers in the II-VI materials[9].

Fig. 4-7 shows the effect on the Hall mobility and the carrier concentration of doping the ablation target at indium concentrations of: 0, $10^{19}/cm^3$, and $10^{20}/cm^3$. The mobilities suggest

a barrier model where transport is by thermionic emission over, and tunneling through, potential barriers.

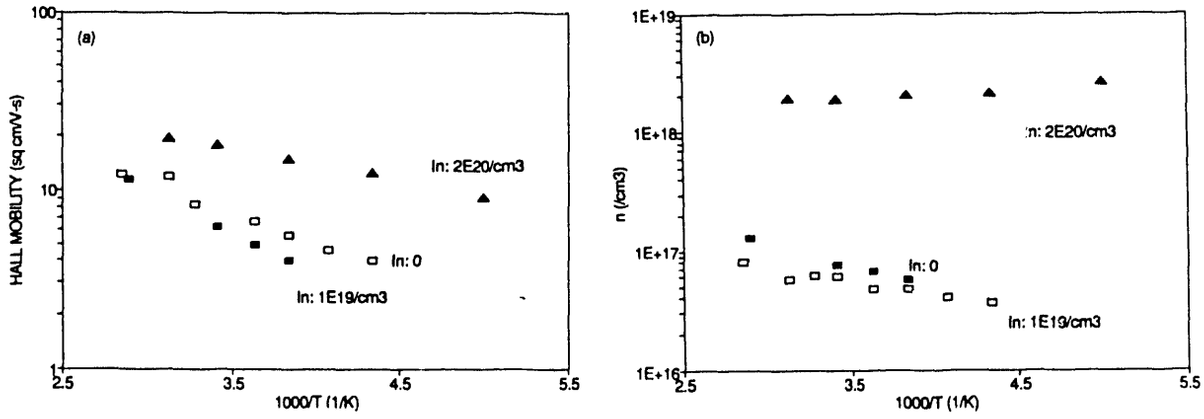

Fig. 4-7. CdS transport properties vs. reciprocal temperature (a) mobility, (b) carrier concentration

One interpretation of the carrier density data is that when the carrier concentration is of the order of $10^{18}/cm^3$ the CdS becomes degenerate[10]. The high temperature activation energy is lower when compared to lower doping concentrations. However, the value for μ_o is also reduced. Thus, doping will raise the conductivity, but this increase is due mainly to an increase in carrier concentration and a lowering of potential barriers at grain boundaries.

Post-Growth Treatments--As an example of the effect of post-growth treatment, sample CSG-19 with a target indium concentration of 500 ppm was dipped in a saturated $CdCl_2$-methanol solution and annealed at 400°C for 20 minutes in air. As a result of this treatment, the resistivity increases, the mobility increases, but the carrier concentration decreases (Fig. 4-8) when compared to the as-grown sample. It should be noted that 4-point probe results imply similar increases in resistivity for CdS treated by improved post-growth treatment techniques. Thus, the treatment of the CdS layer alone should improve cell performance, but this improvement may be more dramatic if the entire cell is treated rather than the individual layers.

Persistent Photoconductivity (PPC) Effects--Residual conductivity effects have been seen in single crystals of CdS for almost 25 years[11,12] over a wide range of temperatures and light exposures. This has included both doped and undoped specimens. It has also been seen in layered materials[13] and mixed crystals[14]. Various mechanisms have been proposed including structural relaxations (DX centers)[15], local potential fluctuations[16], and spatial separation of charge carriers by potential barriers[17]. Each model produces its own time-

dependence for the residual conductivity decay, i.e., a stretched exponential decay[14], a logarithmic decay[17], or a power law relaxation[18]. In many cases all three fits can be used to describe the data. A suitable model to describe the residual conductivity effects could improve our understanding of the conduction mechanisms in these LDPVD films. This could have implications in the development of photovoltaics and optical detectors if it can be determined whether the behavior is intrinsic to the LDPVD CdS or is due to surface states at grain boundaries.

Residual photoconductivity effects were seen in all samples after exposure to low intensity light. A typical curve is shown in Fig. 4-9. These effects were seen over the entire temperature range 80 K - 293 K. The sample response is also a function of wavelength. Four wavelengths were used in this study: 632.8, 514.5, 488 and 457.9 nm. A typical light exposure is 9.4 x 10^{14} photons/$cm^2 \cdot$ s for 600 seconds which is less than 1% of AM1.5 exposure. This type of behavior has also been seen with both weaker and stronger intensities in CdS[11]. A model is currently under development which correlates the conductivity/Hall data with the PPC results. The model suggests that a logarithmic decay of PPC may be appropriate [Fig. 4-9(b)].

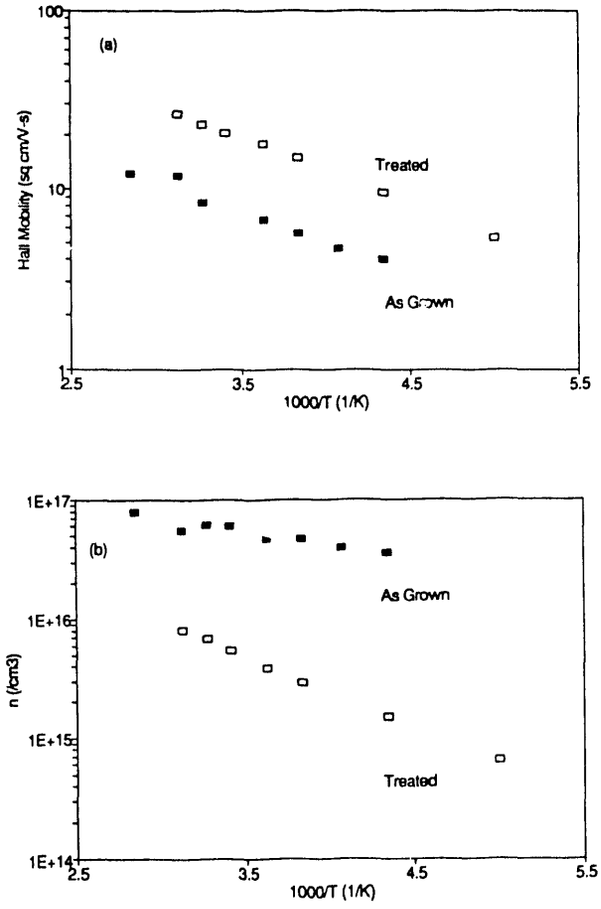

Fig. 4-8. As-grown and treated CdS properties (a) mobility (b) carrier concentation.

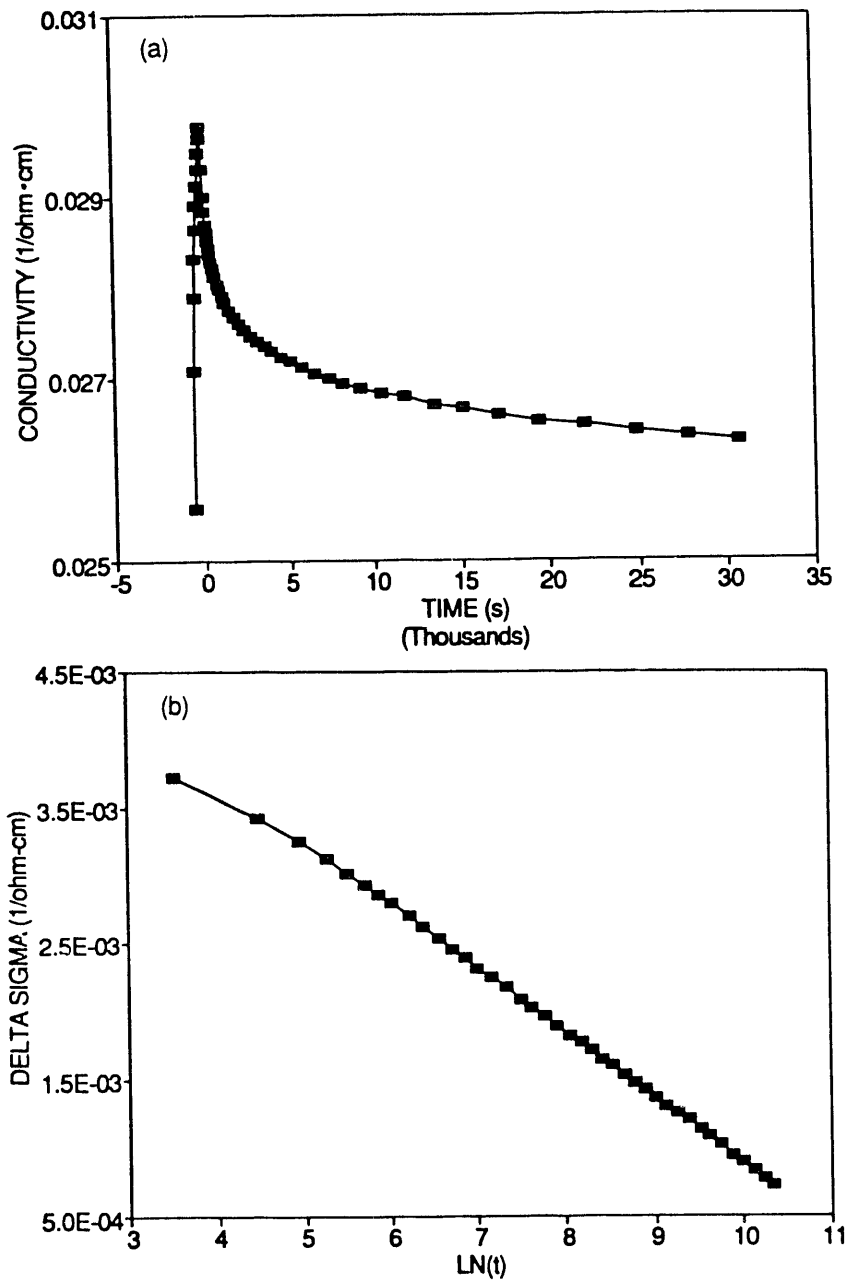

Fig. 4-9. **(a)** Conductivity vs. time during and after exposure to 9.4E14 photons/cm^2·s at 632.8 nm for 10 min; **(b)** logarithmic fit to the decay. The temperature was 293 K.

4.2 LDPVD CdTe

4.2.1 Grain size and film orientation

X-ray Diffraction--The x-ray diffraction peaks shown in Fig. 4-10 indicate that the CdTe grains are preferentially oriented with the cubic <111> direction perpendicular to the substrate. Again, the width of the x-ray peaks were close to the instrumental limit but show some indication of a decreasing width as the substrate temperature was increased.

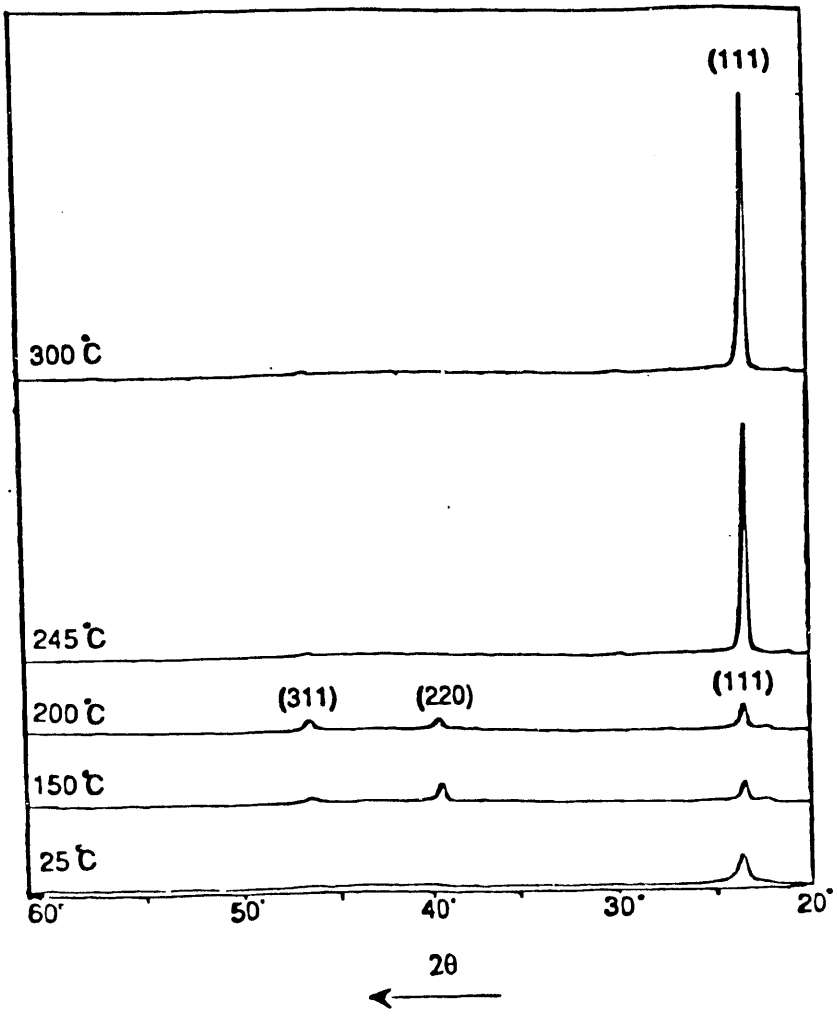

Fig. 4-10. X-ray data for CdTe films deposited at different temperatures.

SEM Studies of CdTe--CdTe films were studied by SEM and EDS before and after several post-growth treatments. The surface texture of as-grown and of $CdCl_2$-treated and annealed CdTe films is presented in Fig. 4-11. Both films were etched for a few seconds in Br-methanol prior to coating with carbon for the SEM. Note that the as-grown LDPVD film on glass is quite smooth on a 1 μm scale but shows some roughness on a scale of 0.1 μm. After annealing at 400°C for 30 minutes in air, the films develop well defined grains with sizes of ~ 1 μm.

(a)

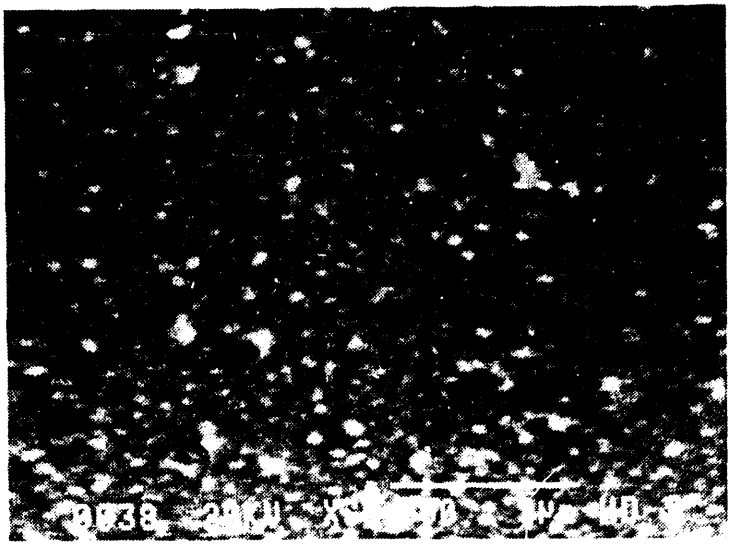

(b)

Fig. 4-11. Surface texture of (a) as grown and (b) treated films

For CdTe on glass substrates, one group of samples was annealed in air after growth, a second group received a thin (two minute deposition) $CdCl_2$ layer by LDPVD and was then annealed, and a third group had a thicker (8 min) $CdCl_2$ deposited before annealing in air. The results for the first and third groups are presented in Fig. 4-12. For a given thickness, and no fluxing agent, the higher the annealing temperature, the larger the grain size. However, at temperatures greater than about 500°C the film sublimes. The fluxing agent $CdCl_2$ effectively lowers the temperatures at which significant grain growth can begin, increasing the atomic mobility during annealing. A two-minute $CdCl_2$ deposition also appears to be sufficient. An even thinner film of $CdCl_2$ might accomplish the same result. Further tests are in progress to determine the minimum $CdCl_2$ thickness for grain growth.

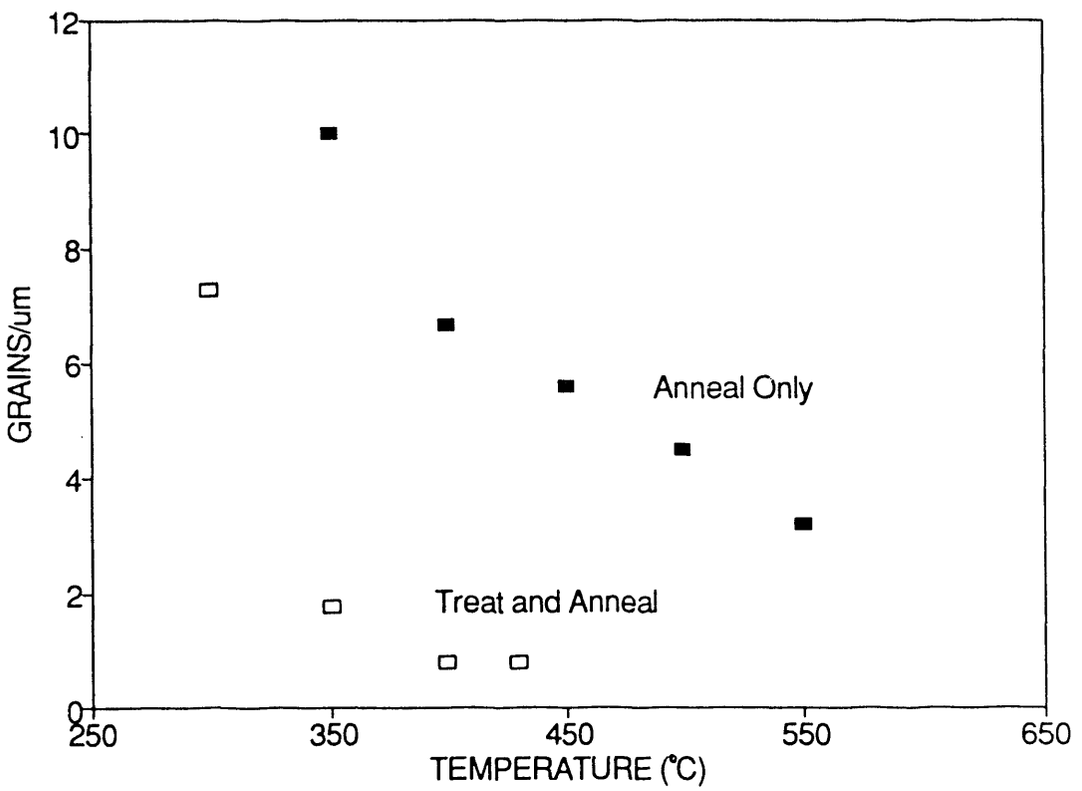

Fig. 4-12. Grain size of CdTe vs annealing temperature for a 1.3 μm film and a 30 minute anneal.

EDS comparisons of spectral intensities for Cd and Te were made using a polished single crystal of CdTe and a film grown at 280 °C. The ratio of the Lα intensities for Te and Cd is 0.674 for the standard and 0.680 for the film. Thus the LDPVD CdTe film is stoichiometric within the experimental uncertainty of $\pm 1\%$.

4.2.2 Optical Properties

Optical absorption measurements on the laser-deposited CdTe films showed that the absorption edge extrapolated from α^2 vs $h\nu$ was $E_g = 1.4$ at room temperature for films deposited at temperatures above ~250°C. At lower deposition temperatures the absorption edge showed significant broadening. Films which were annealed at 400°C without first depositing a layer of $CdCl_2$ showed no change in the absorption edge. However, annealing for 30 to 40 minutes after a laser deposited layer of $CdCl_2$ showed a slight sharpening of the absorption edge and a slight increase in E_g.

Raman scattering was performed with the samples held at liquid nitrogen temperature using Kr laser lines for excitation. The phonon Raman peaks showed clear changes as the deposition temperature increased. The most striking change was the increase in strength and number of overtones. This effect is a result of an increase in carrier lifetime of the free carriers as the film quality improves. The resonant Raman scattering is essentially a resonant fluorescence process in which the laser produces electron-hole pairs which scatter from optical phonons as they thermalize. After each scattering event there is a finite probability of a radiative recombination (fluorescence) process which appears as a Raman peak. However, carrier trapping at impurities and grain boundaries will reduce the carrier lifetime and decrease the strength of the higher order phonon Raman lines. This behavior is clearly seen in the data of Fig. 4-13.

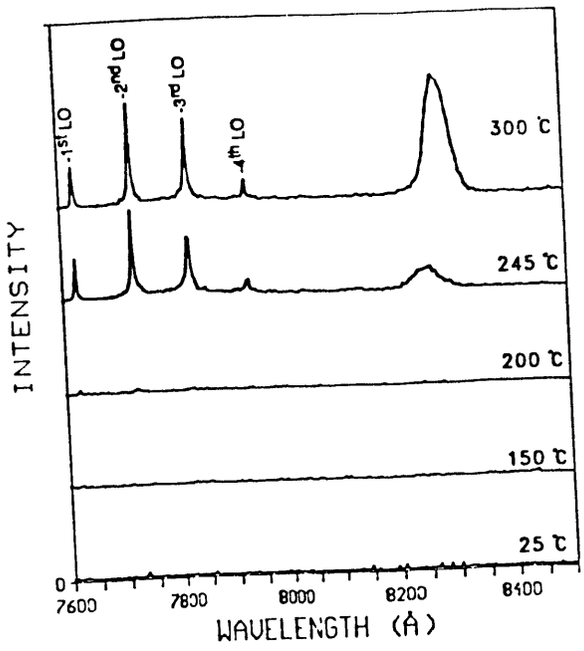

Fig. 4-13. Photoluminescence and Raman peaks from as-grown CdTe films for several growth temperatures. The data were taken at ~10 °K with the $\lambda = 7525$ Å line of a krypton ion laser.

When the carriers thermalize all the way to the band extrema, band-to-band recombination or various impurity-related recombination processes may occur. Fig. 4-14 shows typical luminescence spectra of as-grown and annealed CdTe films. Near-band-edge emission appears at ~7875 Å and the high energy tail of some deep-level recombination appears at the longest wavelengths. Recent work has shown that the use of solid CdTe targets (as opposed to the pressed powder targets) yields stronger near-band-edge emission and decreased deep level emission. Additional studies of the relationship between target structure and film quality will be performed during the second phase of this contract.

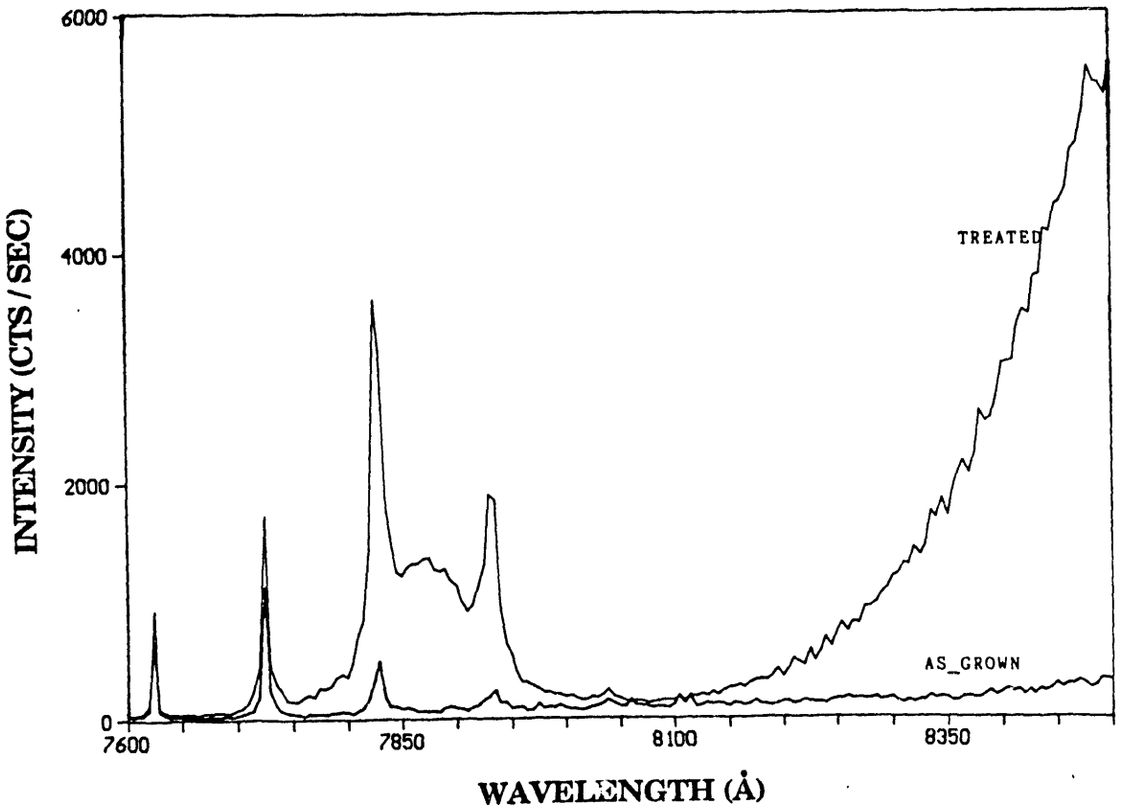

Fig. 4-14. Photoluminescence from as-grown (bottom trace) and treated (top trace) undoped CdTe film at 80 K (Excitation wavelength = 7525 Å; excitation power = 70 mW; growth temperature = 260 °C).

4.2.3 Electrical Transport Properties

Generally, all CdTe samples, doped and undoped, have had in-plane dark resistivities of the order of 10^6 ohm-cm or larger. This is likely due to the tendency of CdTe to self-compensate. Measurement techniques have included Van der Pauw and a striped-electrode configuration. A variety of contacts have been used including Ni-met (a nickel-filled, air-drying polymer from Transene Co. Inc.), graphite, gold, and Cu/Au.

For undoped samples room temperature dark resistivities for as-grown films typically were of the order of 10^9 ohm-cm. Under the solar simulator the in-plane resistivity decreased by approximately two orders of magnitude at room temperature. Films measured early in the project showed some variation in properties (with somewhat lower average dark resistivity at room temperature) from point to point on the film but this improved with a change in deposition parameters.

Post Growth Treatment--Post-growth treatment with $CdCl_2$ does increase the grain size of CdTe but the in-plane resistivity remains high ($\geq 10^6$ ohm-cm at room temperature). However, the resistivity at room temperature decreases by over three orders of magnitude when placed under the solar simulator. This is a significant change compared to the as-grown samples.

Activation energies as obtained from semilogarithmic plots of dark resistivity vs 1/T are of the order of 0.5 eV.

4.3 Sputtered CdTe

DC and RF sputtering are widely used techniques for the deposition of thin films of insulators, semiconductors, and metals. The physical mechanisms of rf magnetron sputtering of solid targets have some similarity to those of LDPVD except that energetic argon ions, typically, are responsible for the target interactions which generate Cd and Te ions and atoms. The sputtered plume is not as tightly directed normal to the target surface as for LDPVD and the typical kinetic energies expected to be ~ 10^2 eV. Again it is a vacuum-based technique. Near the end of the first year we have implemented an rf sputtering system and produced thin films of CdTe on Corning 7059 glass and have incorporated these films in complete solar cell structures. The investigation and optimization of the sputtering process is still in its early stages.

Raman and photoluminescence spectra from two sputtered CdTe films are presented in Fig. 4-15. The film grown at a deposition temperature of 300°C clearly shows better Raman scattering with much enhanced overtones expected for good quality films. The optimization of growth parameters for the sputtered films is still in progress. (Both films of Fig. 4-15 were grown by rf sputtering from a two-inch diameter gun with 90 watts of input power and an argon gas pressure of 5 mTorr.)

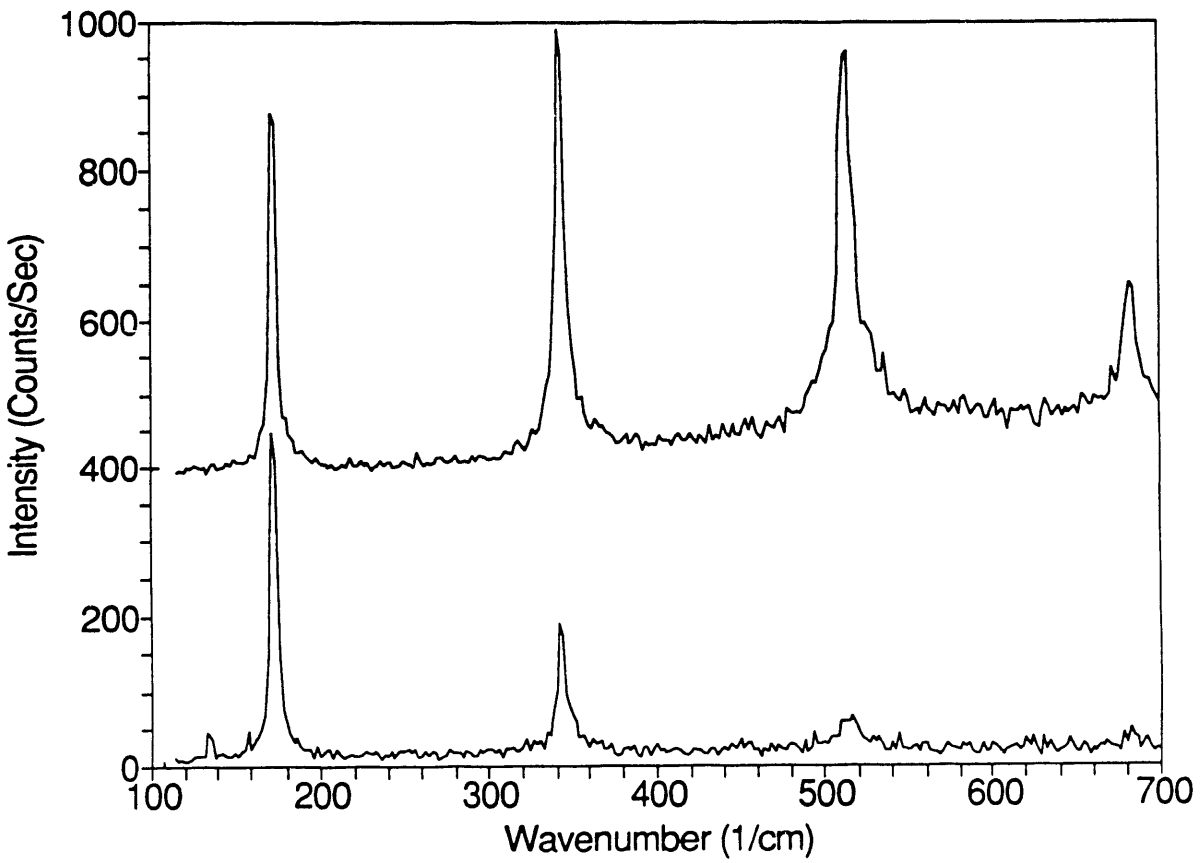

Fig. 4-15. Raman scattering from sputtered CdTe films on glass obtained at liquid nitrogen temperature with λ = 7525 Å. a) growth temperature 250 °C, b) growth temperature 280 °C. Upper trace shifted up by 390 counts for clarity.

4.4 Film stoichiometry and sticking coefficients (ZnTe, CdZnTe, CdS)

Pulsed laser deposition is generally believed to provide a flux of species to the growth surface which closely resembles the target in stoichiometry. This probably accounts for some of its success in the deposition of multicomponent films such as the high temperature superconductors. Of course film stoichiometry also depends on the sticking coefficients of the impinging species. We have examined this behavior in two series of measurements. The first was the determination of the sticking coefficient of Cd and S vs. temperature and the second measurement was the determination of the film stoichiometry of the ternary alloy, CdZnTe.

The average sticking coefficient for a plume of Cd and S was obtained by measuring both the target mass loss and substrate mass increase after a deposition. The sticking coefficients are plotted in Fig. 4-16 as a function of the substrate temperature.

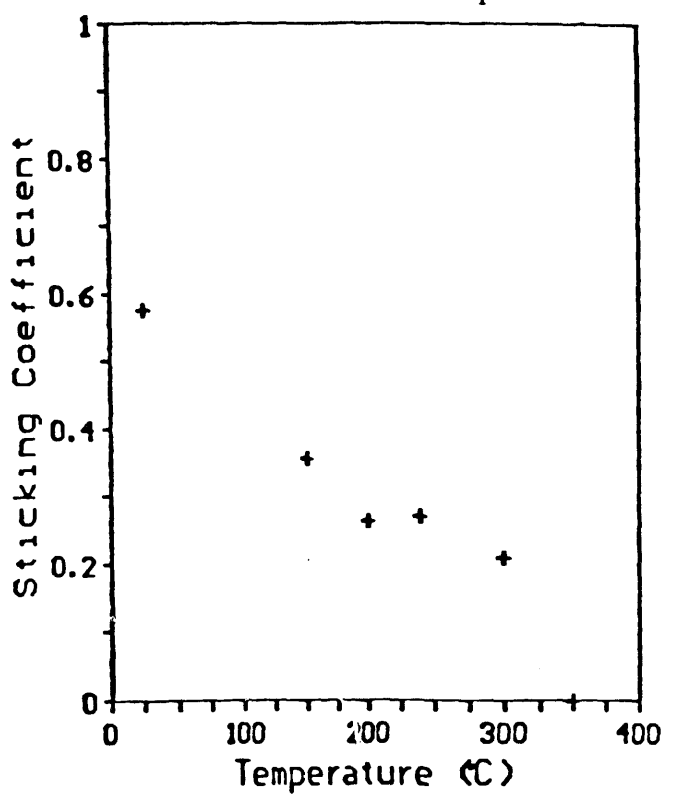

Fig. 4-16. Average sticking coefficient for CdS vs. substrate temperature.

The second set of measurements examined the film stoichiometry of a series of ternary alloys $Cd_xZn_{1-x}Te$. This introduces one constituent which is much lighter in mass than the other two and places no constraint on the Cd:Zn cation ratio in the film. As-grown films were examined with an electron probe for microanalysis (EPMA) by Alice Mason of NREL. The results (See Fig. 4-17.) showed that the films grown at room temperature had a considerable excess of elemental tellurium; however, the films grown at 300°C displayed uniform stoichiometry across the entire film within the errors of the microprobe measurement (2-5%, depending on film thickness) but with a 5 - 35% systematic enrichment of the lighter element Zn over Cd[19].

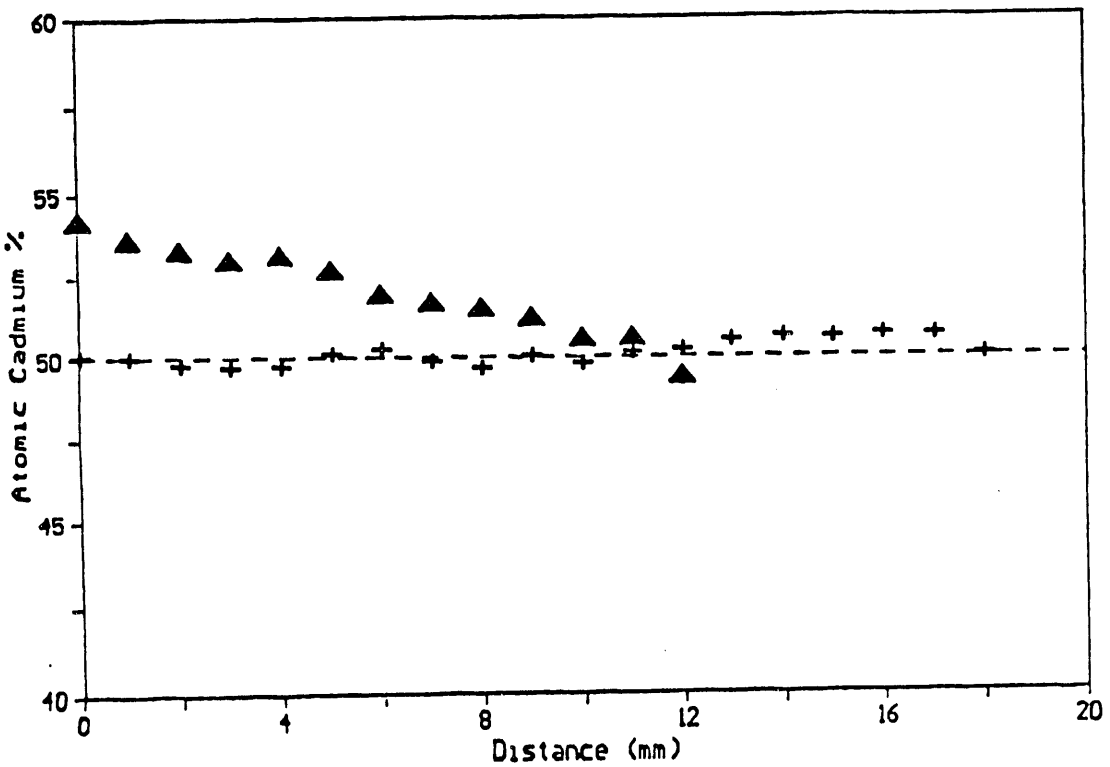

Fig. 4-17. CdS film stoichiometry by EPMA for LDPVD films grown (+) at 300 °C and (▲) at 25 °C. (Data by A. Mason of NREL.)

Doping during LDPVD growth--The use of pressed powder targets facilitates the preparation of target materials such as the ternary alloys described above but also permits the introduction of dopant materials. Thus we have been able to study the effect of doping of ZnTe with Cu over a wide range of dopant concentrations in the target. Cu-doped ZnTe films have been prepared by LDPVD on alkali-free glass (Corning 7059). Measurements of d.c. electrical conductivity were made at room temperature using a strip line geometry. The data (See Fig. 4-18.) show little sensitivity to copper concentration until about 0.3% atomic fraction. Then the resistivity drops by about five orders of magnitude with an increase of a factor of three in Cu concentration in the target. The resistivity of the ZnTe sample with 1% Cu doping in the target was 1 ohm-cm at room temperature. This is consistent with a degenerate semiconductor with a carrier concentration of 10^{18}-$10^{19}/cm^3$. The mobility is less than 3 $cm^2/V \cdot s$ in the temperature range 200-350 K.

A few CdTe samples doped by mixing P or Sb in the target powder have been grown. We have not yet seen that these dopants produce any clear reduction in CdTe resistivity when compared to undoped samples. Other dopants for CdTe will be studied durng the next phase.

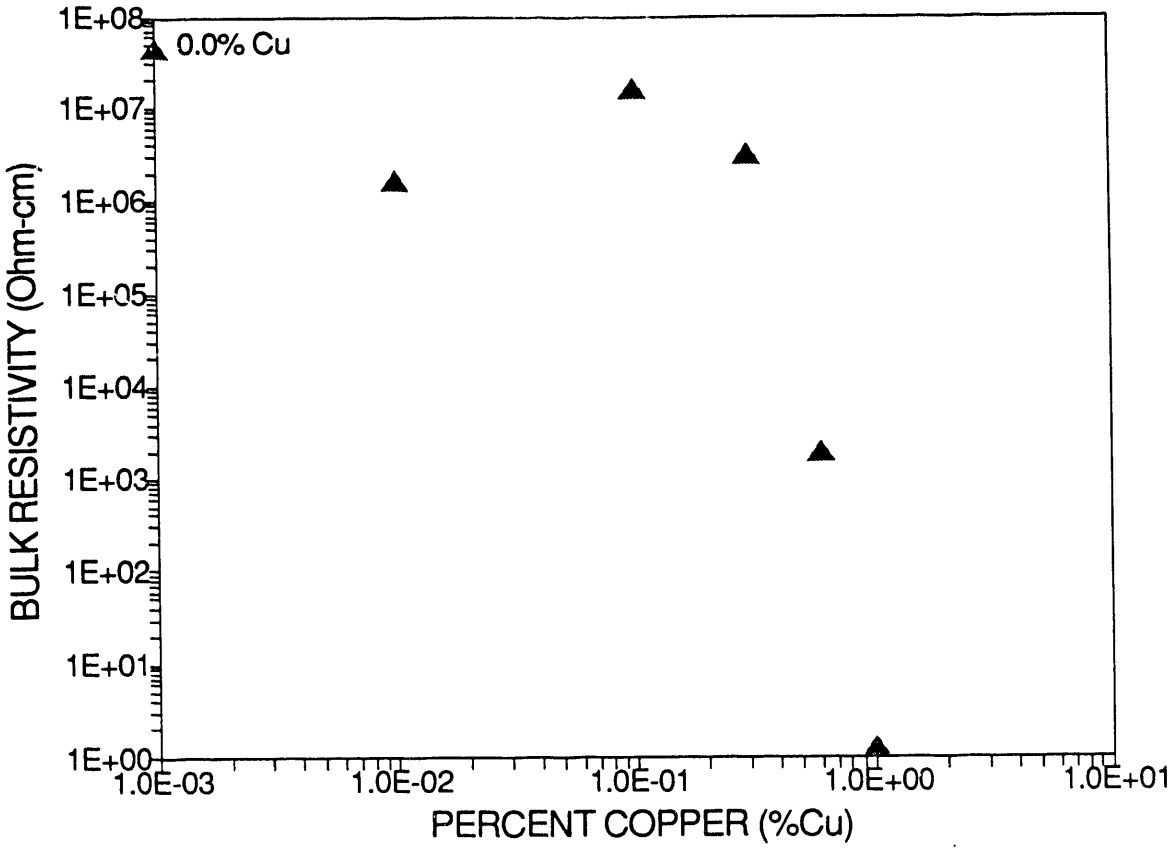

Fig. 4-18. Bulk resistivity of Cu-doped ZnTe as a function of copper percentage.

5.0 Device Fabrication

5.1 n-p structures

As of the end of the first contract year we have found that best cell performance is obtained only after a treatment with $CdCl_2$ followed by annealing at ~400°C. However, we experienced some difficulty in reproducibly applying a thin film of $CdCl_2$ using standard methanol solutions and consequently developed a method for applying the $CdCl_2$ with laser deposition. Thus we have used LDPVD from a pressed target of anhydrous powdered $CdCl_2$ to apply the film in the same vacuum chamber used for the CdS, CdTe and ZnTe film growth. This has proved to be convenient, reproducible, and advantageous for avoiding water contamination.

The I-V characteristic of a recently prepared solar cell is shown in Fig. 5-1. The cell structure was soda-lime glass/SnO_2/CdS/CdTe/Cu/Au. The CdS and CdTe had thicknesses of ~0.3 μm and 1.0 μm respectively, grown by LDPVD. A ~0.2 μm thick layer of LDPVD $CdCl_2$ covered the CdTe. The structure was then annealed at 400°C for 40 minutes prior to evaporation of Cu(~70Å)/Au(130Å) contacts.

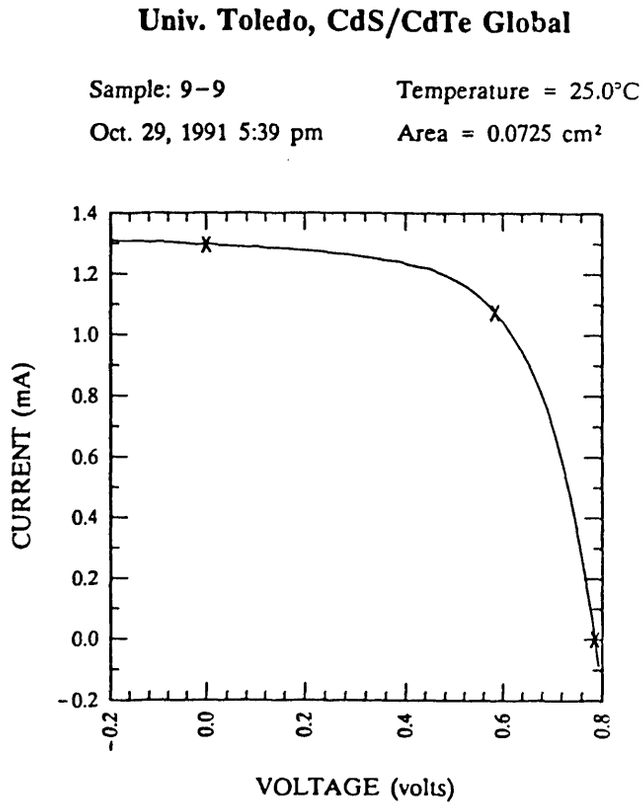

Fig. 5-1. I-V curve as measured by NREL. V_{oc} = 0.786 V, J_{sc} = 17.9 mA/cm^2, P_{max} = 0.628 mW. Fill factor = 61.6%, efficiency = 8.7%

5.2 Minimum CdS window layer thickness

Most of our effort in solar cell fabrication has focussed on the development of reliable and reproducible contacts and on the optimization of the CdTe layer. For the CdS layer, we have used LDPVD targets pressed from both intrinsic CdS powders and from CdS powders doped with 500 ppm of In. We found little difference in the solar cell performance from the different CdS materials undoped or lightly doped with In. Cell performance was found not to depend strongly on the thickness of the CdS for layers greater than 0.5 μm thick. These cell produce essentially no photoresponse below λ = 500 nm. However, we did explore the performance of cells fabricated with much thinner layers of CdS--down to 40-50Å. Fig. 5-2 shows the spectral quantum efficiency for two cells with different CdS thicknesses. Note that at λ < 500 nm the blue response is significantly improved for the ~50 Å CdS layer but in this case the response from the longer wavelength region is significantly degraded. In the second year of this project additional effort will be placed on improving the blue response of the cells with further work on the CdS layer.

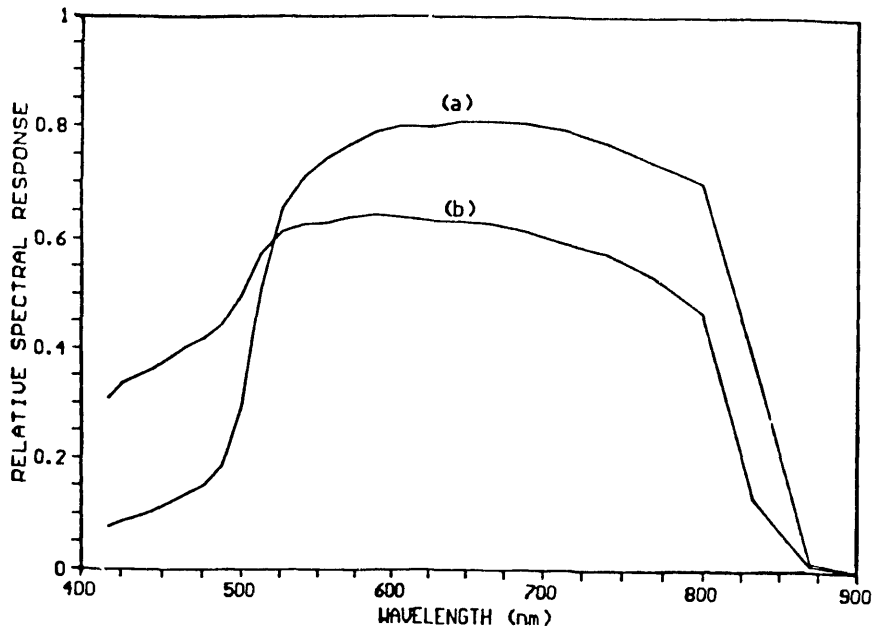

Fig. 5-2. Spectral response curves of (a) sc-130#12, in which the thickness of CdS is 0.15-0.2 μm; and (b) sc-133#5, of which the CdS thickness is 0.05-0.1 μm. Curves (a) and (b) are normalized to the same scale.

5.3 n-i-p structures

Although most of our efforts in cell fabrication were focussed on n-p structures, some results were obtained on n-i-p (CdS-CdTe-ZnTe) structures. The LDPVD system was set up to make sequential depositions of the three semiconductors. In addition, LDPVD was used for $CdCl_2$ depositions. The most promising results were obtained with a $CdCl_2$ deposition after the CdTe deposition. Figure 5-3 provides I-V data for a cell prepared with this n-i-p structure.

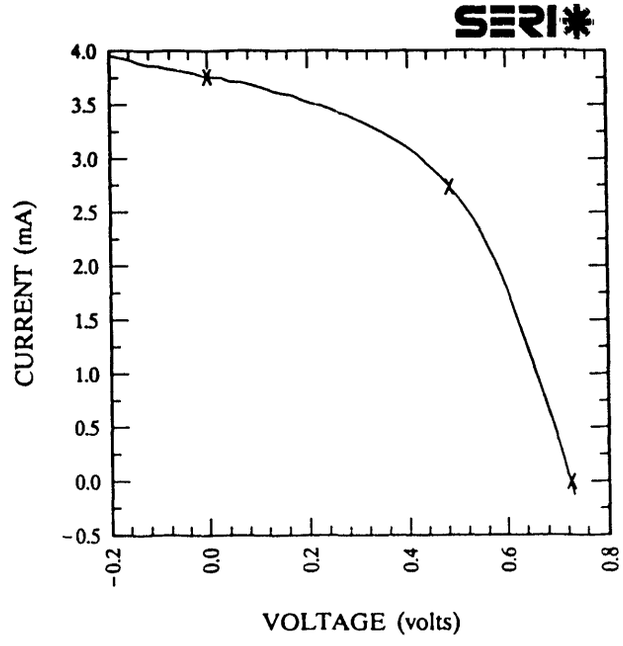

Fig. 5-3. I-V data as measured by NREL for an n-i-p (CdS/CdTe/ZnTe) solar cell prepared by LDPVD.

6.0 Conclusions

First-order optimization of pulsed laser growth of CdS, CdTe, ZnTe, and $CdCl_2$ has been achieved as well as a basic understanding of many of the physical properties of the laser-generated plume. The optimum XeCl laser power density is ~ 3 J/cm^2; target-substrate distances from 5.5 cm to 11 cm have been used successfully; laser wavelengths from 308 nm to 532 nm can be used for the LDPVD; and the optimum substrate temperature is ~ 280 °C.

Complete cell structures have been fabricated with an all LDPVD CdS/CdTe cell delivered and tested by NREL at 8.7% AM1.5. We have found that the LDPVD method is a convenient and reliable technique for applying $CdCl_2$ films in the same vacuum chamber as the semiconductor films.

Initial CdTe depositions have been made with rf sputtering and a sputtered film has been delivered to NREL.

For films grown by the LDPVD process, the thinnest layers of CdS and CdTe which still give good cell performance are ~ 50Å and $\sim 1.0\ \mu$m respectively. These minimum thickness results are being updated as the materials quality improves further.

7.0 Future Directions

During phase one of this contract, major efforts were given to achieving reliable and reproducible depositions of window and absorber layers by both LDPVD and rf sputtering. In addition, we chose to use evaporated Cu/Au contacts for test cells since these were convenient and reproducible. During phase two of this contract, major efforts will be placed on

-improvements in the materials quality of the CdS, CdTe, and ZnTe films,

-controlled introduction of dopants into CdTe and ZnTe to modify the conductivities,

-additional studies of $CdCl_2$ introduced during the deposition process as well as *in situ* annealing,

-studies of alternate contact materials including the use of LDPVD for metallizations to avoid the air exposure,

-optimization of the rf sputtering growth process for CdTe, and

-design issues relating to scale-up of the LDPVD process and the sputtering process to large areas.

These goals will be facilitated by

-systematic studies of low temperature photoluminescence of CdS, CdTe, and ZnTe and comparisons among samples grown by LDPVD, rf sputtering, and other techniques;

-changes in the target preparation including the use of solid and single crystal materials in addition to the pressed powder targets used to date;

-modifications to the growth process to enhance the as-deposited grain size;

-modifications to the LDPVD system to provide more uniform film growth.

We anticipate producing a 12% AM1.5 solar cell by the end of phase two of this project.

8.0 References

1. A. Compaan, R.G. Bohn, A.Aydinli, A. Bhat, L. Tsien, S. Liu, Z. Chen, and C. Tabory, "Thin Film Cadmium Telluride Photovoltaic Cells and Submodules Fabrication," Annual Report, Photovoltaic Program, FY 1990. (March 1991). SERI/TP-211-3643. Available NTIS: Order NO. DE 90000318.

2. A. Compaan, A. Bhat, C. Tabory, S. Liu, M. Nguyen, A. Aydinli, L-H. Tsien, and R.G. Bohn, "Fabrication of CdTe Solar Cells by Laser Driven Physical Vapor Deposition," Solar Cells 30, 79 (1991).

3. B.N. Baron, R.W. Birkmire, J.E. Phillips, W.N. Shafarman, S.S. Hegedus, and B.E. McCandless, "Fundamentals of Polycrystalline Thin Film Materials and Devices" Final Report to SERI July 1990 (Institute of Energy Conversion, Univ. of Delaware, Newark, Delaware, 19716)

4. A. Bhat, Ph.D. Dissertation, "Thin Film Preparation Using Pulsed Laser Deposition," U. of Toledo (1991), unpublished.

5. A. Compaan, A. Bhat, C. Tabory, S. Liu, Y. Li, M.E. Savage, M. Shao, L. Tsien, and R.G. Bohn, Proc. 22nd IEEE Photovoltaic Specialists Conference, Las Vegas, Oct. 7-11, 1991 (to be published).

6. A. L. Fahrenbruch, and R. H. Bube, Fundamentals of Solar Cells, New York, Academic Press 1983, p. 387.

7. N. Nakayama, H. Matsumoto, K. Yamaguchi, S. Ikegami, and Y. Hioki, "Ceramic Thin Film CdTe Solar Cell," Jpn. J. Appl. Physics, 15, 2281)1976).

8. Y. K. Jun and H. B. Im, "Effect of Thickness and Sintering Conditions of CdS Films on the Photovoltaic Properties of CdS/CdTe Solar Cells," J. Electrochem. Soc., 135, 1658 (1988).

9. L. D. Partain, G. J. Sullivan, and C. E. Birchnall, "Effects of Indium on the Electrical Properties of n-type CdS," J. Applied Physics, 50, 551 (1979).

10. I. A. Karpovich and B. N. Zvonkov, "Hall Mobility of Electrons in Cadmium Sulfide and Selenide Films," Soviet Physics - Solid State, 6, 2714 (1965).

11. H. C. Wright, R. J. Downey, and J. R. Canning, "Conductivity Storage in CdS," J. Phys. D, 1, 1593 (1968).

12. I. V. Markevich, G. A. Fedorus, and M. K. Sheinkman, "High-Temperature Residual Conductivity of CdS(Ag), CdS(Au), and CdS(Na) Crystals," Sov. Phys. Semicond., 3, (1970).

13. H. J. Queisser and D. E. Theodorou, "Hall-Effect Analysis of Persistent Photocurrents in n-GaAs Layers," Phys. Rev. Letters, 43, 401 (1979).

14. H. X. Jiang and J. Y. Lin, "Persistent Photoconductivity and Related Critical Phenomena in $Zn_{0.3}Cd_{0.7}Se$," Phys. Rev., B40, 10025 (1989).

15. M. Housin, M. Fialin, G. Sagnes, G. Bastide, and M. Rouzeyre, "Physical Properties of the Deep X Electron Trap Responsible for Long Time Persistent Photocapacitance in CdS, Physica, 118B, 155 (1983).

16. M. K. Sheinkman and A. Y. Shik, "Long-term Relaxation and Residual Conductivity of Semiconductors (review)," Sov. Phys. Semicond., 10, 128 (1976).

17. H. J. Queisser and D. E. Theodorou, "Decay Kinetics of Persistent Photoconductivity in Semiconductors," Phys. Rev., B33, 4027 (1986).

18. R. Pandya and E. A. Schiff, "Differential Photocurrent Transient Measurements in a-Si:H," J. Noncrys. Sol., 59, 297 (1983).

19. A. Aydinli, A. Compaan, G. Contreras-Puente, and A. Mason, "Polycrystalline $Cd_{1-x}Zn_xTe$ Thin Films on Glass by Pulsed Laser Deposition," Sol. State Commun. **80**, 465 (1991).

9.0 Publications

Refereed papers published:

1. A. Compaan, A. Bhat, C. Tabory, S. Liu, M. Nguyen, A. Aydinli, L-H. Tsien, and R. G. Bohn, "Fabrication of CdTe Solar Cells by Laser-Driven Physical Vapor Deposition," Solar Cells, 30, 79, 1991.

2. A. Aydinli, G. Contreras Puente, A. Bhat, and A. Compaan, "$ZnSe_xTe_{1-x}$ Films Grown by Pulsed Laser Deposition," J. Vac. Sci. & Technol. (accepted for publication 7/1/91).

3. A. Aydinli, A. Compaan, G. Contreras-Puente and Alice Mason, "Polycrystalline $Cd_{1-x}Zn_xTe$ Thin Films on Glass by Pulsed Laser Deposition," Sol. St. Commun. (1991), (accepted for publication 8/25/91).

4. A. Compaan, A. Bhat, C. Tabory, S. Liu, Y. Li, M.E. Savage, M. Shao, L. Tsien, and R.G. Bohn, "Polycrystalline CdTe Solar Cells by Pulsed Laser Deposition," Proc. 22nd IEEE Photovoltaic Specialists Conference p. 957 (1992) [Las Vegas, NE, Oct. 1991].

Annual Reports published in SERI Annual Report, Photovoltaic Subcontract Program:

1. A. Compaan, R.G. Bohn, A.Aydinli, A. Bhat, L. Tsien, S. Liu, Z. Chen, and C. Tabory, "Thin Film Cadmium Telluride Photovoltaic Cells and Submodules Fabrication," Annual Report, Photovoltaic Program, FY 1990. (March 1991). SERI/TP-211-3643. Available NTIS: Order NO. DE 90000318.

2. A. Compaan, R.G. Bohn, A. Aydinli, A. Bhat, C.N. Tabory, L. Tsien, S. Liu, M. Shao, M.E. Savage, and Y. Li, "Thin Film Cadmium Telluride Photovoltaic Cells," Annual Report, Photovoltaic Program, FY 1991. (to be published)

Papers and Talks presented:

A. K. Bhat, A. D. Compaan, R. G. Bohn, L. Tsien, C. Tabory, Bull. Am. Phys. Soc. 35, 714 (1990). "Thin Film Deposition of CdS Using Pulsed-Laser Evaporation."

A. Compaan, A. Aydinli, C. Tabory, S-Z Liu and M. Nguyen, Bull. Am. Phys. Soc. 35, 714 (1990). "Structural and Optical Properties of ZnTe Deposited by Laser Ablation Deposition."

J. F. Knudsen, P. M. Adams, R. C. Bowman, Jr., and A. D. Compaan, Bull. Am. Phys. Soc. 35, 820 (1990). "Effects of Laser Annealing on Si Ion Implanted GaAs."

L. Tsien, R. G. Bohn and A. D. Compaan, The Ohio Section Meeting of the Amer. Phys. Soc. (November 1990), "Electrical Transport Properties of Polycrystalline CdS Films Produced by Laser Ablation Deposition."

S. Liu, A. Bhat, C. Tabory, and A. D. Compaan, The Ohio Section Meeting of the Amer. Phys. Soc. (November 1990) "Spectral Quantum Efficiency (SOE) Measurements of CdS/CdTe Thin-film Solar Cells,"

A. Aydinli and A. Compaan, Bull Am. Phys. Soc. 36, 397 (1991). "Epitaxial Deposition of ZnTe and ZnSe and GaAs by Laser-Driven Physical Vapor Deposition."

A. Compaan, H. D. Yao, P. M. Adams, J. F. Knudsen and R. C. Bowman, Jr., Bull. Am. Phys. Soc. 36, 543 (1991). "Topical Studies (Raman and X-ray) of Heavily Implanted, Laser Annealed n-GaAs."

L. Tsien, R. G. Bohn and A. D. Compaan, Bull. Am. Soc. Phys. 36, 960 (1991). "Residual Conductivity in Polycrystalline CdS Films."

Z. Chen, A. Aydinli, G. Contreras-Puente, A. K. Bhat and A. Compaan, Bull. Am. Phys. Soc. 36, 1036 (1991). "Pulsed Laser Deposition of $ZnSe_x$ Te_{1-x} and $Cd_xZn_{1-x}Te$ Thin Films."

A. Bhat, S. Liu, C. Tabory, M. Nguyen, A. Aydinli and A. Compaan," Bull. Am. Phys. Soc. 36, 1037 (1991). "CdTe/CdS Solar Cells by Laser-Driven Physical Vapor Deposition."

S. Liu, A. K. Bhat, C. Tabory and A. Compaan, Bull. Am. Phys. Soc. 36, 1037 (1991). "Spectral Quantum Efficiency of CdS/CdTe Thin-Film Solar Cells Grown by Pulsed Laser Deposition."

10.0 Students and Visitors Participating in the Project

Students:

Ajit Bhat Ph.D. March 1992	"Thin Film Preparation Using Pulsed Laser Deposition"
Mai Nguyen M.S. April 1991	"Photoluminescence and Raman Scattering from CdTe and CdS Films Grown by Laser-Driven Physical Vapor Deposition"
Shuzhen Liu M.S. Feb. 1991	"Spectral Quantum Efficiency Measurements in CdTe/CdS Solar Cells"
Ph.D. in progress	
Marc Savage M.S. in progress	
Yuxin Li M.S. in progress	
Li-Hua Tsien Ph.D. in progress	"Electrical Transport Properties and Residual Conductivity in CdS Films Grown by Laser-Driven Physical Vapor Deposition"
Meilun Shao M.S. in progress	"SEM and EDS Studies of II-VI Semiconductor Films Grown by Laser-Driven Physical Vapor Deposition"

Technical Assistants:

Charles N. Tabory

Nicolas Lavalle (part-time)

Visiting Scientists:

Prof. Atilla Aydinli from Beyteppe Univ. Ankara, Turkey (Aug-Sept, 1991)

Dr. Michael Tamor from the Physics Department, Ford Motor Company, Dearborn, MI (Sept-Oct, 1991)

Document Control Page	1. NREL Report No. NREL/TP-451-4797	2. NTIS Accession No. DE92001239	3. Recipient's Accession No.

4. Title and Subtitle

Thin Film Cadmium Telluride Photovoltaic Cells

5. Publication Date

April 1992

6.

7. Author(s)

A. Compaan and R. Bohn

8. Performing Organization Rept. No.

9. Performing Organization Name and Address

University of Toledo
Department of Physics and Astronomy
Toledo, OH 43606

10. Project/Task/Work Unit No.

PV231101

11. Contract (C) or Grant (G) No.

(C) ZN-1-19019-3

(G)

12. Sponsoring Organization Name and Address

National Renewable Energy Laboratory
1617 Cole Blvd.
Golden, CO 80401-3393

13. Type of Report & Period Covered

Technical Report
23 July 1990 - 31 October 1991

14.

15. Supplementary Notes

NREL technical monitor: B. von Roedern

16. Abstract (Limit: 200 words)

This report describes research to develop two vacuum-based growth techniques for CdTe thin-film solar cells: (1) laser-driven physical vapor deposition (LDPVD) and (2) radio-frequency (rf) sputtering. The LDPVD process was successfully used to deposit thin films of CdS, CdTe, and $CdCl_2$, as well as related alloys and doped semiconductor materials. The laser-driven deposition process readily permits the use of several target materials in the same vacuum chamber and, thus, complete solar cell structures were fabricated on SnO_2-coated glass using LDPVD. The rf sputtering process for film growth became operational, and progress was made in implementing it. Time was also devoted to enhancing or implementing a variety of film characterization systems and device testing facilities. A new system for transient spectroscopy on the ablation plume provided important new information on the physical mechanisms of LDPVD. The measurements show that, e.g., Cd is predominantly in the neutral atomic state in the plume but with a large fraction that is highly excited internally ($\geq$ 6 eV), and that the typical neutral Cd translational kinetic energies perpendicular to the target are 20 eV and greater.

17. Document Analysis

a. Descriptors

thin films ; cadmium ; telluride ; photovoltaics ; solar cells

b. Identifiers/Open-Ended Terms

c. UC Categories

273

18. Availability Statement

National Technical Information Service
U.S. Department of Commerce
5285 Port Royal Road
Springfield, VA 22161

19. No. of Pages

42

20. Price

A03

Form No. 0069E (6-30-87)